Investigation of the effect of posttranslational modification of lipoproteins in TLR2-mediated recognition of *Staphylococcus aureus*

Doctoral thesis

to obtain a doctorate (Dr. med.)

from the Faculty of Medicine

of the University of Bonn

Justus Mann

from Kassel

2025

Written with authorization of

the Faculty of Medicine of the University of Bonn

First reviewer: Prof. Dr. Isabelle Bekeredjian-Ding

Second reviewer: Prof. Dr. Gabriele Bierbaum

Day of oral examination: 21.08.2025

From the Institute for Medical Microbiology, Immunology and Parasitology

Table of contents

List of abbreviations

aa	amino acid
agr	accessory gene regulator
amp	ampicillin
AST	antimicrobial susceptibility testing
BCA	bicinchoninic acid
bp	base pairs
CA-MRSA	community-associated MRSA
CC	clonal complex
cDNA	copy deoxyribonucleic acid
CF	cystic fibrosis
CHO cells	chinese hamster ovary cells
CO_2	carbon dioxide
C_T	cycle threshold
ddATP	dideoxyadenosine 5′-triphosphate
ddNTPs	dideoxynucleotide triphosphates
DMEM	Dulbecco's Modified Eagle Medium
DNA	deoxyribonucleic acid
DNase	deoxyribonuclease
dNTPs	deoxynucleotide triphosphates
dsDNase	double-strand specific deoxyribonuclease
E. coli	*Escherichia coli*
EDTA	ethylenediaminetetraacetic acid
ELISA	enzyme-linked immunosorbent assay
EUCAST	European Committee on Antimicrobial Susceptibility Testing
FBS	fetal bovine serum
G+C	guanine + cytosine
Geh	glycerol ester hydrolase
H_2O_2	hydrogen peroxide

H_2SO_4	sulfuric acid
HA-MRSA	health care-associated MRSA
HEK293 cells	human embryonic kidney 293 cells
IL-8	interleukin-8
LA-MRSA	livestock-associated MRSA
Lgt	preprolipoprotein diacylglyceryl transferase
LipA	lipoic acid synthetase
LnsA	lipoprotein N-acyl transferase system A
LnsB	lipoprotein N-acyl transferase system B
Lnt	N-acyltransferase
LPS	lipopolysaccharide
Lsp	prolipoprotein signal peptidase
MALDI-TOF	matrix-assisted laser desorption ionization–time of flight
MIC	minimal inhibitory concentration
MLST	multilocus sequence typing
mRNA	messenger ribonucleic acid
MRSA	methicillin-resistant *S. aureus*
MSSA	methicillin-sensitive *S. aureus*
MUSCLE algorithm	multiple sequence comparison by log-expectation algorithm
MyD88	myeloid differentiation primary response 88
Na_2CO_3	sodium carbonate
NaCl	sodium chloride
$NaClO_4$	sodium perchlorate
$NaHCO_3$	sodium hydrogencarbonate
NaOH	sodium hydroxide
NCBI	National Center for Biotechnology Information
NOD	nucleotide-binding oligomerization domain
OD	optical density

PAMPs	pathogen-associated molecular patterns
PBP	penicillin binding protein
PBP2a	penicillin-binding-protein 2a
PBS	phosphate-buffered saline
PCR	polymerase chain reaction
pH	potential of hydrogen
PVL	Panton-Valentine leukocidin
rcf	relative centrifugal force
RFU	relative fluorescence units
RIPA buffer	radioimmunoprecipitation assay buffer
RNA	ribonucleic acid
rpm	revolutions per minute
r_s	spearman correlation coefficient
RT-PCR	reverse-transcription polymerase chain reaction
S. aureus	*Staphylococcus aureus*
SAv-HRP	streptavidin-horseradish peroxidase conjugate
SCC*mec*	staphylococcal chromosome cassette *mec*
SCV	small colony variant
SDS	sodium dodecyl sulphate
SLV	single locus variant
SNP	single nucleotide polymorphism
SSSS	*staphylococccal* scaled skin syndrome
ST	strain type
T	thymine
T/S	trimethroprim/sulfamethoxazole
TLR	Toll-like receptor
TMB	tetramethylbenzidine
TSB	tryptic soy broth

1 Introduction

1.1 *Staphylococcus aureus*

Staphylococcus aureus (*S. aureus*) is an opportunistic pathogen for humans and animals. Although around 30 % of the healthy population is colonized with *S. aureus*, it can cause severe, life-threatening infections (H. Wertheim et al., 2005). The significance of the pathogen becomes clear by comparing the mortality rate of *S. aureus* bacteremia with deaths due to other infectious diseases. The annual mortality rate of *S. aureus* bacteremia is higher than the combined mortality rates of acquired immune deficiency syndrome, tuberculosis and viral hepatitis (van Hal et al., 2012). Figure 1.1 shows *S. aureus* grown on Columbia Blood Agar plates.

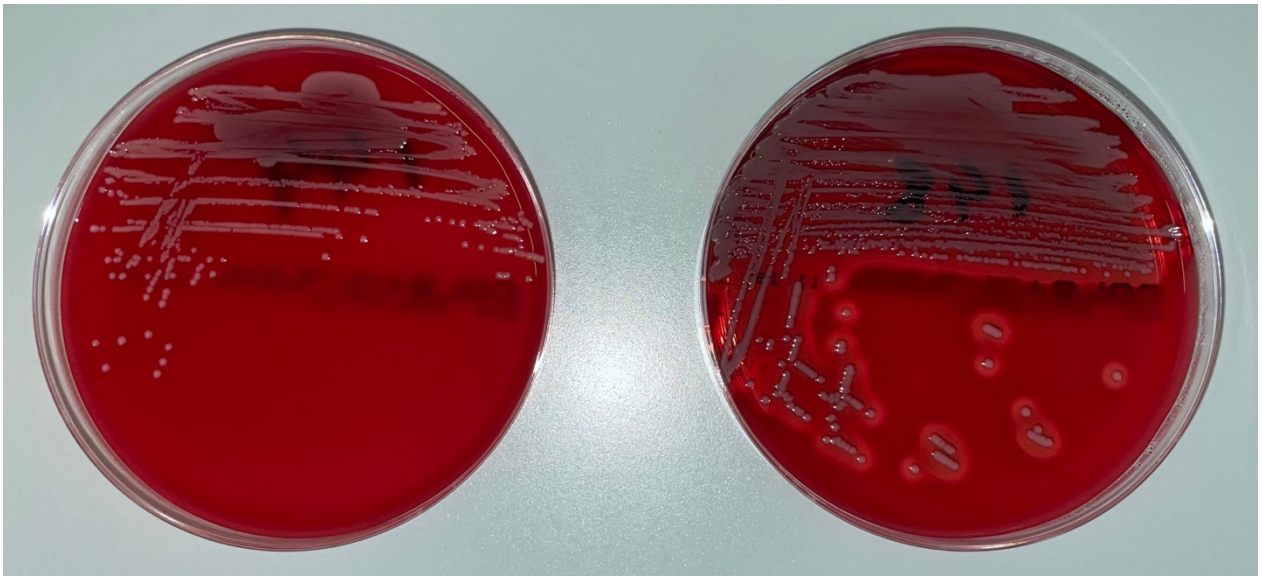

Figure 1.1: Two different *S. aureus* isolates from this work grown on Columbia Agar with Sheep Blood Plus plates (Thermo Fisher Scientific, Massachusetts, USA). The left plate shows isolate INV144 as an example of a non-hemolytic strain. The right plate shows isolate INV148 with typical beta-hemolysis around the colonies. Colonies from both isolates are grey to white. Other isolates' colonies are rather yellow giving the species its name (from Latin "aureus" = golden).

1.1.1 Transition from colonizing bacterium to disease-causing pathogen

Commensal *S. aureus* can be located everywhere on the skin or mucosae but is preferentially localized in the anterior nares. A successful eradication by the immune system is possible,

since studies differentiate between persistent carriage, intermittent carriage and non-carriage. Furthermore, the percentage of colonization in children is significantly higher than in adults, indicating the successful elimination of the commensal pathogen. In the case of an infection, the strain isolated from the infection site is often identical with the colonizing strain. Colonization with *S. aureus* is therefore a risk factor for endogenous infections (H. Wertheim et al., 2005). Interestingly, non-carriers with bacteremia showed a higher mortality rate compared to carriers (of who 80% were endogenously infected) (H. F. L. Wertheim et al., 2004). Whether the better infection outcome in carriers is due to an improved, previously existing, immune response or due to the relative harmlessness of colonizing strains remains unclear. Much research is currently focused on better understanding the interaction of the host and the pathogen as well as the mechanisms of colonization, outbreak of infection and eradication of the pathogen.

1.1.2 Diseases caused by *S. aureus*

The variety of diseases caused by *S. aureus* is enormous. The bacterium can cause invasive infections in basically every organ system. Infections range from local skin and soft tissue infections to urinary tract infections, device-associated infections, bone and joint infections, endocarditis and pneumonia, just to name a few. All infections pose the potential to develop into life-threatening sepsis and shock. *S. aureus* strains can produce a number of toxins that increase the severity of infections (cytotoxic toxins, e.g., hemolysins, Panton-Valentine leukocidin) or cause diseases themselves (superantigens). Superantigens activate T-cells in an antigen-independent manner, subsequently causing excessive immune activation in severity ranging from light nausea to life-threatening shock. Examples are staphylococcal enterotoxins causing food poisoning and the toxic shock syndrome toxin 1 causing the toxic shock syndrome. Another toxin-caused disease is staphylococcal scalded skin syndrome evoked by exfoliative toxins. Although these toxins play a crucial role in the initiation and establishment of infections, they are not the focus of this project and are just mentioned for the sake of completeness (Lowy, 1998; van Hal et al., 2012).

1.1.3 *S. aureus* in cystic fibrosis patients

Cystic fibrosis (CF) patients differ in their carriage rate of *S. aureus* from healthy individuals. The airways of CF patients are often chronically infected with various microbes. In many children, *S. aureus* is the first detected pathogen in early childhood, followed usually by *Pseudomonas aeruginosa*. While eradication of a recently acquired *S. aureus* infection is successful in most cases, the success decreases with prolonged time of carriage leading to high rates of persistent, chronic *S. aureus* infections among CF patients. Chronic *S. aureus* infection can lead to the formation of small colony variants (SCVs). SCVs differ in many things compared to regular *S. aureus* (e.g., smaller colonies on agar plates and a decreased susceptibility for antibiotics). However, the four *S. aureus* isolates from CF patients in this work are not SCVs (Goss & Muhlebach, 2011).

1.1.4 β-lactam antibiotics in the treatment of *S. aureus*

β-lactam-antibiotics are a broad class of agents effective against Gram-negative and Gram-positive bacteria, including *S. aureus*. Their bactericidal effect occurs through binding to and thereby inactivating penicillin binding proteins (PBPs). PBPs are enzymes involved in bacterial cell wall formation. β-lactams can be subdivided into penicillins (e.g., the first clinically used β-lactam penicillin G, the first β-lactamase-stable penicillin methicillin, or the penicillin used in this work ampicillin), cephalosporins and carbapenems. Another subclass are monobactams. However, they do not play a role when talking about *S. aureus* since they are not effective against Gram-positive bacteria (Bush & Bradford, 2016).

Gain of β-lactam-resistance mainly derives from two different mechanisms. In one mechanism, strains possessing the enzyme β-lactamase are resistant to most of the penicillins. β-lactamases inactivate penicillins by hydrolysis of their eponymous β-lactam ring. In the other mechanism, strains contain the gene *mecA*. *mecA* encodes the alternate penicillin-binding-protein 2a (PBP2a) and confers resistance to almost all β-lactam-antibiotics. PBP2a is a PBP variant with low affinity for β-lactams, that continues cell wall formation even when treated with β-lactam-antibiotics. *mecA* is part of a mobile cassette element leading to the term “Staphylococcal chromosome cassette *mec*” (SCC*mec*). Historically, PBP2a was first described as conferring resistance against the β-lactam-drug

methicillin, a semi-synthetic penicillin with intrinsic resistance against β-lactamases. Albeit PBP2a confers resistance against almost all β-lactam-antibiotics, strains producing PBP2a are classified as methicillin-resistant *S. aureus* (MRSA). Strains that do not encode *mecA* are referred to as methicillin-susceptible *S. aureus* (MSSA). Two cephalosporins, ceftobiprole and ceftaroline, show a much higher affinity to PBP2a and are therefore effective in the treatment of MRSA (Chambers & DeLeo, 2009).

MRSA strains can be further categorized by their origin: health care-associated MRSA (HA-MRSA), community-associated MRSA (CA-MRSA) and livestock-associated MRSA (LA-MRSA) (Köck et al., 2011). However, this distinction has not been done for the clinical MRSA isolates analyzed in this work.

Interestingly, subinhibitory concentrations of β-lactam antibiotics have been shown to increase the pathogenicity of MRSA by upregulating the expression of lipoprotein-like genes. Lipoprotein-like proteins triggered proinflammatory cytokines through the activation of TLR2 (Shang et al., 2019).

1.2 Staphylococcal lipoproteins

Bacterial lipoproteins are a class of membrane-bound proteins encoded by 1-3 % of bacterial genes. Lipoproteins are present on the cell surface and are involved in a variety of functions such as nutrient-acquisition, cell wall construction, protein maturation and antibiotic resistance. Lipoproteins therefore are essential not only for bacterial growth, but also invasion and survival in infection sites. The membrane attachment of lipoproteins is highly conserved across bacterial species, thus lipoproteins are the main ligands for Toll-like receptor 2 and can reveal the presence of an infection to the host innate immune system. These properties make lipoproteins an interesting topic of current studies (Nakayama et al., 2012; Schmaler et al., 2010).

1.2.1 N-terminal lipidation anchors lipoproteins to the bacterial cell membrane

Lipoproteins are different from other membrane proteins in that they contain no transmembrane amino acid sequences in their mature form. Instead, the otherwise

hydrophilic protein is anchored to the hydrophobic bacterial cell membrane by fatty acids covalently attached to its N-terminus. Currently, five different N-terminal modifications have been described for the anchoring of lipoproteins (Figure 1.2): di-acylated lipoproteins (N-acylation-free S-diacyl-glyceryl-cysteine), tri-acylated lipoproteins (N-acyl-S-diacyl-glyceryl-cysteine), lyso lipoproteins (N-acyl-S-monoacyl-glyceryl-cysteine), N-acetyl lipoproteins (N-acetyl-S-diacyl-glyceryl-cysteine) and peptidyl lipoproteins (N-X-X-S-diacyl-glyceryl-cysteine) (Kurokawa, Ryu, et al., 2012; Nakayama et al., 2012).

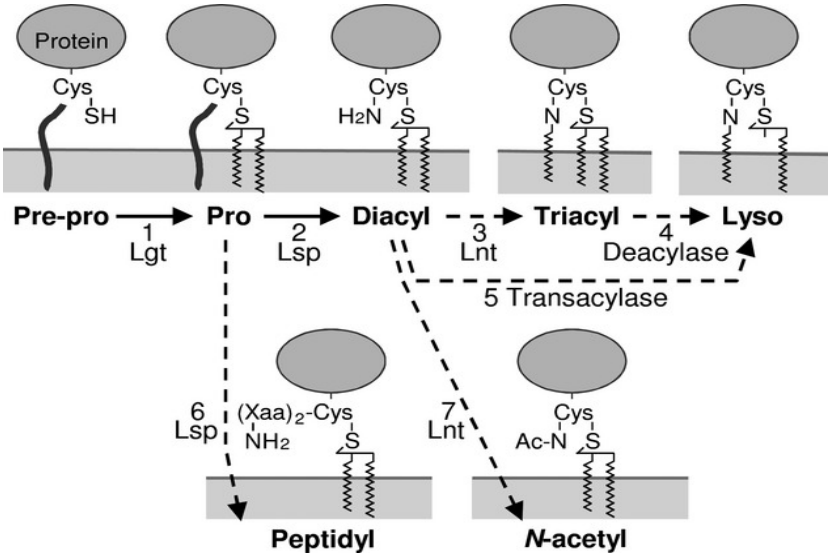

Figure 1.2: Synthesis pathways of the different lipoprotein lipidation states. The FEBS Journal, Volume: 279, Issue: 23, Pages: 4247-4268, First published: 25 October 2012, DOI: (10.1111/febs.12041) (Nakayama et al., 2012)

Gram-negative bacteria usually synthesize tri-acylated lipoproteins as they use the third fatty acid as a means to recognize and sort the lipoprotein to the outer membrane. Thus, the mechanism of N-terminal lipidation has been best studied in the Gram-negative bacterium *Escherichia coli* (*E. coli*). In the first lipidation step, preprolipoprotein diacylglyceryl transferase (Lgt) adds a diacylglycerol to the thiol side chain of the N-terminal cysteine. Prolipoprotein signal peptidase (Lsp) removes the signal peptide from the newly acylated protein. The resulting apolipoprotein (= di-acylated lipoprotein) is the substrate for apolipoprotein N-acyltransferase (Lnt), which adds a fatty acid to the amino group of the N-

terminal cysteine creating the hololipoprotein (tri-acylated lipoprotein) (Nakayama et al., 2012).

Low G+C containing Gram-positive Bacteria (*Firmicutes*), including *S. aureus*, are lacking the enzyme Lnt, which has been discovered to perform N-acylation on *E. coli* lipoproteins (Asanuma et al., 2011). Gardiner et al. discovered two *S. aureus* genes being together sufficient to perform N-acylation on lipoproteins: *lnsA* (SAOUHSC_00822) and *lnsB* (SAOUHSC_02761). Their given names derive from their function: Lipoprotein N-acyl transferase system (Lns) (Gardiner et al., 2020).

1.2.2 *S. aureus* changes lipoprotein lipidation due to environmental changes

Unlike *E. coli*, *S. aureus* changes the proportion of lipoprotein di- and tri-acylation depending on the environmental conditions and growth phase. Most other bacterial species studied to date do not do this, and rather carry out only one type of lipoprotein-modification for a uniformly acylated lipoprotein population (for example *E. coli*) or modify each lipoprotein in a specific matter (for example *Mycoplasma fermentans*) (Kurokawa, Ryu, et al., 2012). In principle, *S. aureus* has the ability to uniquely di- or tri-acylate every lipoprotein. In exponential-growth phase, lipoproteins were mainly tri-acylated regardless of pH value (pH 6 - 7.5). In post-logarithmic-growth phase, decreasing the pH from 7.5 to 6 caused a shift from tri-acylated lipoproteins towards their di-acylated counterparts. Increasing the temperature from 37 °C to 42 °C increased the amount of di-acylated lipoproteins as well. An increased salt concentration (7.5 % NaCl compared to 1 % NaCl) accelerated the effect in low pH and high temperature but did not induce a shift itself. The observed shift in N-terminal lipoprotein-lipidation required functioning protein synthesis and was therefore not caused by converting tri- to di-acylated lipoproteins by hydrolysis (Asanuma et al., 2011; Kurokawa, Kim, et al., 2012).

S. aureus has several ways to sense environmental changes (e.g., a drop in pH or an increase in salt concentration) and react to them. A common mechanism are two-component systems: An extracellular signal leads to the autophosphorylation of a histidine kinase, which further phosphorylates and activates a response regulator. This response regulator can

induce and repress the expression of genes involved in bacterial virulence. Most strains possess 16 two-component systems of which one is obligatory (WalRK) and the other 15 can be mutated (A. Wertheim, 2019). Interestingly, all 15 mutants synthesized tri-acylated lipoproteins at pH 7.5 and di-acylated lipoproteins at pH 6.0 in post-exponential-growth phase. The changes in the lipoprotein lipidation do not seem to be caused by two-component systems (Kurokawa, Kim, et al., 2012).

1.3 Toll-like receptors

Toll-like receptors (TLRs) are part of the innate immune system. They bind to a variety of molecules derived from pathogens including bacteria (PAMPs: pathogen-associated molecular patterns). Different TLRs recognize different PAMPs. For example, TLR4 plays a crucial role in the detection of Gram-negative bacteria by sensing lipopolysaccharide (LPS). However, due to their lack of LPS, TLR4 is not predominantly detecting Gram-positive bacteria like *S. aureus*. Instead, one of the main TLRs recognizing Gram-positive bacteria is TLR2, through its recognition of lipoprotein acylation (Takeuchi et al., 1999).

1.3.1 TLRs responsible for the detection of *S. aureus*

In vivo murine infection models showed the important role of TLR2 in initiating an appropriate immune response against *S. aureus*. TLR2-deficient mice infected with *S. aureus* were more susceptible to the infection and showed an increased mortality compared to wild-type mice (Takeuchi et al., 2000). For a while, peptidoglycan was postulated to be one of the main staphylococcal ligands binding to TLR2. However, peptidoglycan was found to activate cells via NOD receptors, and the main TLR2 agonists were determined to be lipoproteins (Tawaratsumida et al., 2009). Previously tested peptidoglycan fractions, along with other postulated TLR2 ligands, were presumably contaminated with lipoproteins. *In vitro* infection models showed the necessity of mature lipoproteins in activating TLR2. A Δ*lgt S. aureus* mutant, which fails to add any acyl chains to the immature lipoprotein, did not induce TLR2 signaling (Kurokawa et al., 2009).

TLR2 associates with additional receptors to allow recognition of a wide variety of molecules. Tri-acylated lipoproteins induce heterodimerization of the ectodomains of human TLR2 and

TLR1. The two fatty acids esterified to the glycerol at the N-terminal end of the lipoprotein are located inside a hydrophobic pocket of TLR2. The third, amide linked, acyl chain is located inside a hydrophobic channel of TLR1. The lipoprotein thereby brings both TLRs and therefore their carboxy termini close together which initiates intracellular signaling cascades and results in an inflammatory response (Jin et al., 2007). The synthetic ligand Pam_3CSK_4 binds TLR2/1 as a mimic of this process.

Di-acylated lipoproteins induce heterodimerization of the extracellular domains of TLR2 and TLR6. The two fatty acids esterified to the glycerol are located inside a hydrophobic pocket of TLR2, just like mentioned above. TLR6 does not contain a lipid channel like TLR1 since the channel-equivalent is distinctly narrowed. The amide linked acyl chain on tri-acylated lipoproteins would not fit inside which explains the receptor's specificity for di-acylated lipoproteins. Although di-acylated lipoproteins are lacking the third complex-stabilizing fatty acid, stable complex formation is still possible. The peptide head group bridges both TLRs via hydrogen bonds. Furthermore, the protein-protein interactions between TLR2 and TLR6 are stronger due to an increased hydrophobic dimerization interface. Connected via the peptide headgroup of di-acylated lipoproteins, TLR6 and TLR2 ectodomains come together which initiates, as mentioned above, intracellular signaling cascades and results in an inflammatory response (Kang et al., 2009). $Pam_2\,CSK_4$ binds TLR2/6 as a synthetic ligand.

Since tri-acylated lipoproteins signal through TLR2/1 and their di-acylated counterparts signal through TLR2/6, the detected signal can be used in a reporter assay as an indicator for the lipoprotein lipidation state. Deleting *lnsA* or *lnsB* in *S. aureus* decreased the TLR2/1 signal while the TLR2/6 signal stayed unaffected, indicating the loss of tri-acylated lipoproteins. Deleting *lgt* or *lsp* decreased, as expected, TLR2/1 and TLR2/6 signal, since only maturated lipoproteins can signal though TLRs. The expected change in lipidation was further confirmed using matrix-assisted laser desorption ionization–time of flight (MALDI-TOF) mass spectrometry. *Listeria monocytogenes* naturally synthesizes di-acylated lipoproteins. However, inserting *lnsA* and *lnsB* into *Listeria monocytogenes* strongly increased the TLR2/1 signal indicating the presence of previously absent tri-acylated lipoproteins. Inserting just one

gene did not change the TLR2/1 signal suggesting both genes, *lnsA* and *lnsB*, are together necessary to perform N-acylation on lipoproteins (Gardiner et al., 2020).

As well as distinguishing between TLR2's dimerization partner, the lipidation state affects the immune activating potential through TLRs in general. Stimulating cells that are expressing TLR2, TLR6 and TLR1 on their cell surface with heat-killed bacteria showed differences in the signal intensity due to different lipoprotein lipidation states. Di-acylated lipoproteins induced the strongest signal, followed by their tri-acylated counterparts. The lyso-form induced the weakest signal (Gardiner et al., 2020).

Although TLR2 heterodimerized with TLR1 or TLR6 is an important part of the innate immune system when faced with *S. aureus*, other receptors seem to be involved as well. To initiate the signaling cascade, TLR2 is dependent on the adapter protein MyD88. Murine infection models with TLR2-deficient and MyD88-deficient mice showed an increased mortality compared to wild-type. However, the effect was stronger in the MyD88-deficient mice compared to the TLR2-deficient mice suggesting other MyD88-dependant receptors can recognize *S. aureus* as well (Takeuchi et al., 2000).

1.3.2 Common polymorphism of TLR1 affects its trafficking to the cell surface

Not surprisingly, over time, a variety of single nucleotide polymorphisms (SNPs), have derived within the genes encoding human TLRs. In some cases, the SNP causes a change in the amino acid sequence, in other cases it does not. The potential clinical relevance of a TLR polymorphism is determined for one thing by the chemical properties of the changed amino acid, for another thing by the localization of the amino acid within the protein structure. One TLR1 polymorphism, that is firstly very common and secondly shows a strong effect on the receptor's function, is of interest for this work and therefore further elaborated: The reference sequence of human TLR1 consists of a Serine at position 602 (TLR1 602S). It is the predominant allele among western Europeans. Interestingly, TLR1 602S does not traffic to the cell surface and therefore does not recognize tri-acylated lipoproteins or Pam_3CSK_4. However, TLR1 602S has been presumed to play a protective role against leprosy, an infectious disease caused by *Mycobacterium leprae*. By contrast, TLR1 602I, that consists of

the single nucleotide polymorphism 1805G>T, resulting in an amino acid change from Serine to Isoleucine at position 602 (Ser602Ile), is present on the cell surface and sufficiently detects tri-acylated lipoproteins as well as Pam_3CSK_4 (Johnson et al., 2007; Skevaki et al., 2015). Nonetheless, this “sufficient” TLR1 602I phenotype is rare among the white European population. According to the National Center for Biotechnology Information (NCBI) SNP (rs) report, the 602S allele (rs5743618) has a prevalence of almost 70 % in Europe (n = 21994), compared to under 20 % in Africa (n = 3554) (National Center for Biotechnology Information, 2022).

1.3.3 *S. aureus* masks its lipoproteins from recognition by TLR2

Interestingly, *S. aureus* has the ability to evade immune recognition by TLR2. Since detection by TLR2 is dependent on the esterified fatty acids on bacterial lipoproteins, hydrolyzing the ester-bound fatty acids on secreted lipoproteins masks them from recognition by TLR2. The secreted *S. aureus* lipase glycerol ester hydrolase (Geh) has long been known to act on mammalian lipids. Recently published data revealed the enzyme’s ester hydrolase activity on endogenous lipoproteins. *In vitro* data showed Geh’s ability to inactivate TLR2 ligands and *in vivo* data showed an accelerated immune response and an improved clearance in mice infected with Δ*geh S. aureus* (Chen & Alonzo, 2019). The lipase Geh therefore seems to play a crucial role in the interplay between *S. aureus* lipoproteins and the innate immune system.

1.4 Aim of this study

S. aureus has been postulated to change its lipoprotein acylation patterns under varying environmental conditions. Whether lipoproteins are posttranslationally di- or tri-acylated results in differences in recognition by human Toll-like receptors. In 2012, Kurokawa et al. observed a shift from tri- to di-acylated *S. aureus* lipoproteins by growth in a decreased pH environment in the stationary phase of growth. The underlying mechanisms, especially the genes involved in tri-acylation of *S. aureus* lipoproteins, were unknown at that time. Eight years later, Gardiner et al. discovered that two genes *lnsA* and *lnsB* encoded enzymes responsible for tri-acylation. LnsA and LnsB activity decreased bacterial recognition by TLR2 and shifted its dimerization partner from TLR6 to TLR1.

Based on these findings, the aim of this study was to investigate whether *S. aureus*-mediated posttranslational lipoprotein modification under stress conditions is conserved across the *S. aureus* species. In particular, we hypothesized that regulation of *lnsA* and *lnsB* expression under stress conditions results in altered TLR2 recognition and immunogenicity, which could account for host adaptation of *S. aureus* to colonization and infection.

2 Materials and methods

2.1 Characterization of bacterial isolates

A collection of 30 different *S. aureus* isolates from different origins was examined as part of this work. Table 2.1 provides an overview of the isolates' origins and caused diseases. The isolates were previously described by Hilmi et al. (Hilmi et al., 2014; Hilmi, 2013; Hilmi, 2010). Two reference strains used were USA300, a community-associated MRSA strain and SA113, an *agr* mutant derived from NCTC 8325. Both strains were kindly provided by Prof. Friedrich Götz, Tübingen. Two isolates from healthy adults were obtained from a study on nasal carriage (ethics commission approval protocol 208/15 at the University of Frankfurt, Germany).

Table 2.1: Origins and caused diseases of the *S. aureus* isolates studied in this work

Isolate	Sample Material	Diagnosis
CF014	nasal polyp tissue	sinusitis
CF018	sputum	-
CF031	throat swab	-
CF173	sputum	-
FB002	nose swab	asymptomatic carriage
FB004	nose swab	asymptomatic carriage
INV001	mitral valve tissue	endocarditis
INV005	bone tissue	osteomyelitis
INV058	blood culture	endocarditis
INV075	blood culture	-
INV078	urine	urinary tract infection
INV091	paranasal sinus tissue	-
INV099	abscess swab	abscess
INV100	wound swab	wound
INV101	urine	urinary tract infection
INV108	wound swab	wound
INV109	tracheal secretion	pneumonia/bronchitis
INV117	unknown material in blood culture bottle (from right upper leg)	-
INV120	blister swab	suspected SSSS / varicella infection superinfected with *S. aureus*
INV130	blood culture	-
INV144	surgical mastoid swab	-
INV148	intraarticular knee tissue	
INV162	tissue	necrotizing fasciitis
INV172	blood culture	suspected sepsis
INV179	abscess swab	abscess
INV195	foot tissue	diabetic foot
INV198	tricuspid valve tissue	endocarditis
INV202	blood culture	suspected meningitis

2.1.1 Genotypic characterization of the *S. aureus* isolate collection

To investigate on the virulence of the isolates, a quadruplex PCR was performed targeting *nuc*, *mecA*, *mecALGA251* and Panton-Valentine leucocidin (*luk-PV*). Primers and probes were used as described by Pinchon et al. (Pichon et al., 2012).

Bacteria were grown on Columbia Agar with Sheep Blood Plus plates (Thermo Fisher Scientific, Massachusetts, USA). Three single colonies were picked for each strain and diluted in 500 µL 0.9% NaCl (Fresenius Kabi Deutschland GmbH, Bad Homburg, Germany). Samples were boiled for five minutes at 95 °C. Multiplex PCR was performed using the Biozym Probe qPCR Mix Separate ROX (Biozy, Scientific GmbH, Hessisch Oldendorf, Germany). Reactions were prepared as described in Table 2.2.

Table 2.2: PCR reaction mix for the real-time quadruplex PCR assay

Reagent	**Volume (µL) for 20 µL reaction**
Probe qPCR 2xMix (containing DNA polymerase, buffer and dNTPs)	10
Primer: Nuc F 100 µM	0.1
Primer: Nuc R 100 µM	0.1
Primer: PVL F 100 µM	0.1
Primer: PVL R 100 µM	0.1
Primer: mecA F 100 µM	0.1
Primer: mecA R 100 µM	0.1
Primer: mecC F 100 µM	0.1
Primer: mecC R 100 µM	0.1
Probe: Nuc FAM 100 µM	0.25
Probe: PVL CY5 100 µM	0.25
Probe: mecA HEX 100 µM	0.25
Probe: mecC ROX 100 µM	0.25
Nuclease-Free Water (Promega GmbH, Walldorf, Germany)	4.1
Sample	5

PCR was performed as described in Table 2.3 using the MIC Magnetic Induction Cycler (Bio Molecular Systems, Upper Coomera, Australia) and software micPCR v2.12.7 (Bio Molecular Systems, Upper Coomera, Australia).

Table 2.3: Protocol for the real-time quadruplex PCR assay

Reaction	Time (s)	Temperature (°C)	Repeats
Initial Denaturation	120	95	1
Denaturation	5	95	40
Annealing/Extension	30	60	

All 30 isolates tested positive via PCR for the *nuc* gene, a species-specific housekeeping gene, confirming all isolates as *S. aureus*. 12 isolates harbored the *mecA* gene and were classified as MRSA. Those isolates encoded the alternate penicillin-binding protein PBP2a conferring resistance to most β-lactam-antibiotics. No isolate tested positive for $mecA_{LGA251}$, also termed *mecC.* Notably, $mecA_{LGA251}$ is a homologue of *mecA*, sharing approximately 70 % nucleotide homology. It is associated with livestock infections and other veterinary infections (Paterson et al., 2012). Furthermore, four isolates tested positive for Panton-Valentine leucocidin (PVL), a pore forming toxin that kills human leukocytes and is associated with severe skin infections and necrotizing pneumonia (van Hal et al., 2012). USA300 was used as a positive control for *mecA* and *luk-PV* (An Diep et al., 2006; Tenover et al., 2006). SA113 was used as a negative control. PCR results for every isolate are shown in Table 2.4.

Table 2.4: Multiplex-PCR results for the *S. aureus* isolate collection

***S. aureus* isolate**	**Gene**			
	nuc	***mecA***	***mecA*$_{LGA251}$**	***luk-PV***
CF014	+	-	-	-
CF018	+	-	-	-
CF031	+	+	-	-
CF173	+	+	-	-
FB002	+	-	-	-
FB004	+	+	-	-
INV001	+	+	-	-
INV005	+	+	-	-
INV058	+	-	-	-
INV075	+	+	-	-
INV078	+	+	-	-
INV091	+	-	-	+
INV099	+	-	-	-
INV100	+	-	-	-
INV101	+	-	-	-
INV108	+	-	-	-
INV109	+	-	-	-
INV117	+	-	-	-
INV120	+	-	-	-
INV130	+	+	-	-
INV144	+	-	-	-
INV148	+	-	-	-
INV162	+	-	-	-
INV172	+	-	-	-
INV179	+	+	-	+
INV195	+	+	-	-
INV198	+	-	-	-
INV202	+	+	-	+
SA113	+	-	-	-
USA300	+	+	-	+

2.1.2 Detection of PBP2a protein in MRSA, but not MSSA isolates

The collection of 30 isolates consisted of 18 MSSA isolates and 12 MRSA isolates according to the *mecA* PCR. To determine if *mecA* was expressed and if *mecA* positive isolates contained the PBP2a protein, an antigen test was performed. MRSA isolates were tested individually, MSSA isolates were pooled in groups of five or six isolates as shown in Table 2.5. USA300 and SA113 were not tested as part of this work as they have been well-characterized elsewhere.

Table 2.5: Pooling of MSSA isolates in three groups

Pool 1 (5 isolates)	**Pool 2 (6 isolates)**	**Pool 3 (6 isolates)**
FB002	INV091	INV109
INV101	INV099	INV148
INV117	INV100	INV162
INV120	INV108	INV172
CF014	INV144	INV058
	CF018	INV198

The presence of PBP2a protein in each isolate was determined using the Clearview™ PBP2a SA Culture Colony Test (Abbott Laboratories, Chicago, USA) according to the manufacturer's protocol. Figure 2.1 shows the results of the PBP2s antigen test. All pooled MSSA strains tested negative, confirming the absence of PBP2a. Ten out of 11 predicted MRSA isolates were clearly positive for PBP2a. The exception was FB004. FB004 encoded *mecA* but was only slightly positive for PBP2a in the antigen test.

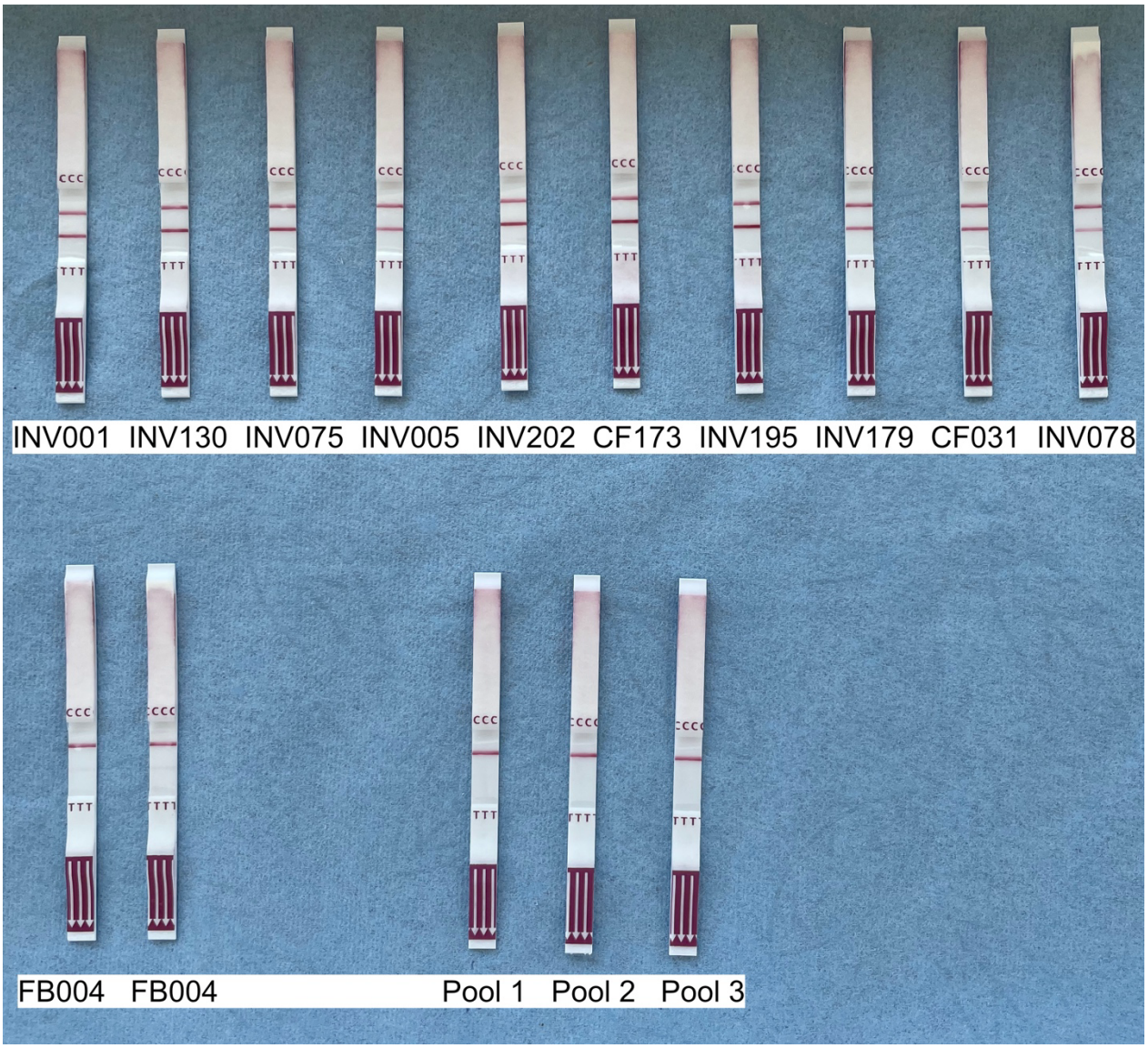

Figure 2.1: Detection of PBP2a protein in MRSA isolates. PBP2a antigen tests were performed on *S. aureus* isolates. The ten isolates tested in the upper row were all clearly positive for PBP2a. The lower row shows isolate FB004 tested twice with an ambiguous result, as well as the pooled MSSA isolates all testing negative.

Because of the ambiguous result, FB004 was tested again confirming the slightly positive result. FB004 was further cultured on a selective agar plate using a chromogenic medium (CHROMagar MRSA / CHROMagar Staph. Aureus pre-poured plates (bi-plates), MAST Diagnostica GmbH, Reinfeld, Germany). It did not grow on the MRSA selective agar, despite detection of *mecA* by PCR. Isolate INV078 is shown as a MRSA control (Figure 2.2).

Genomically, isolate FB004 was a MRSA strain, while phenotypically, and therefore clinically, it behaved like a MSSA strain.

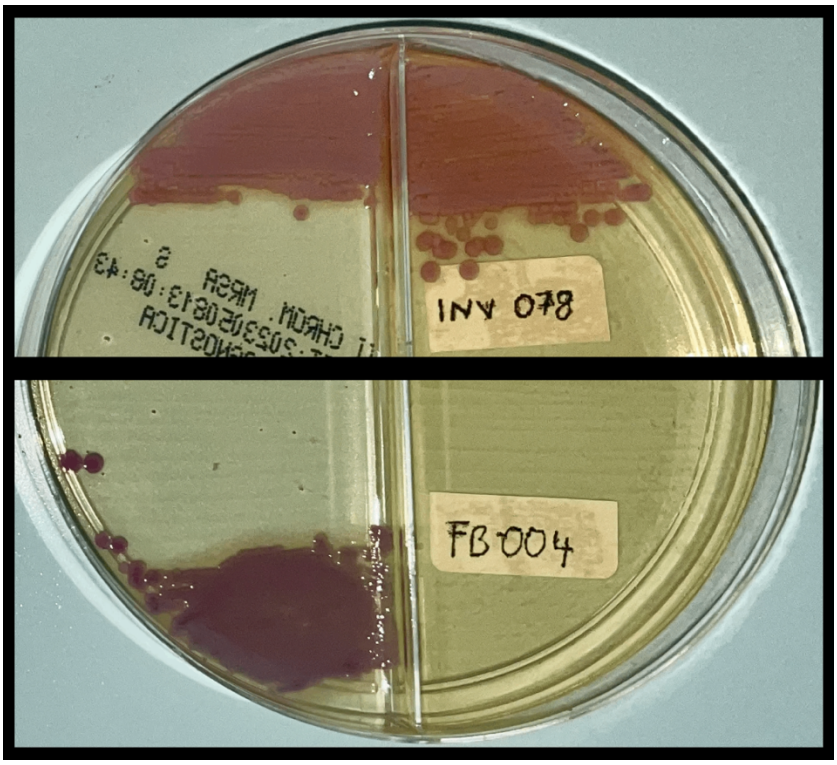

Figure 2.2: Isolates INV078 (upper plate) and FB004 (lower plate) grown on selective agar plates. The left half of the plate enables the differentiation of *S. aureus* from other bacteria by colour. *S. aureus* grows in pink-ish colours while other bacterias' colonies appear colourless, blue or inhibited. Pink-ish growth on the right side of the plate confirms an isolate as MRSA. Growth of MSSA strains is inhibited. According to the manufacturer, the MRSA detection rate has a sensitivity and specificity close to 100 %.

2.1.3 Antimicrobial susceptibility testing (AST) of the 28 clinical *S. aureus* isolates

Antimicrobial susceptibility was further examined by a minimal inhibitory concentration (MIC) assay (MICRONAUT-S MRSA/GP system, MERLIN Gesellschaft für mikrobiologische Diagnostika mbH, Bornheim-Hersel, Germany). Testing was performed on the 28 clinical isolates only. Bacteria were grown on Columbia Agar with Sheep Blood over night at 37°C. Single colonies were picked and inoculated in NaCl 0.45 % (VITEK 2.0 0.45% SALINE BAG, bioMérieux, Inc., Durham, North Carolina, USA) until the bacterial suspension reached 0.55

- 0.63 McFarland. 100 µL of the bacterial suspension were transferred into 11.5 mL Mueller Hinton Broth, cation adjusted (CAMHB) (MERLIN Gesellschaft für mikrobiologische Diagnostika mbH, Bornheim-Hersel, Germany). A 96-well plate, on which each well contained a different antibiotic concentration, was inoculated with 100 µL per well. The plate was sealed and incubated for 20 hours at 37 °C. Read out was performed using the Multiskan FC Microplate Photometer (Thermo Fisher Scientific, Massachusetts, USA) and MICRONAUT-Software (MERLIN Gesellschaft für mikrobiologische Diagnostika mbH, Bornheim-Hersel, Germany). Breakpoints were defined by EUCAST (The European Committee on Antimicrobial Susceptibility Testing, 2023: Breakpoint tables for interpretation of MICs and zone diameters. Version 13.1, 2023. http://www.eucast.org (access date:19.11.2023)).

Table 2.6 shows the results of the β-lactam antibiotics benzylpenicillin, ampicillin, oxacillin, cefoxitin and ceftaroline. 24 out of 28 isolates tested resistant to penicillin and ampicillin. Ten of those isolates, the ones positive for PBP2a protein, showed additional resistance to oxacillin and cefoxitin, which function as MRSA-screening antibiotics. According to this MIC-testing, isolate FB004 was a MSSA strain, even though it encoded *mecA*.

Table 2.6: Antibiotic susceptibility testing of β-lactam antibiotics determined by minimal inhibitory concentration testing. R = resistant; I = intermediate; S = susceptible.

	CF014	CF018	CF031	CF173	FB002	FB004	INV001	INV005	INV058	INV075	INV078	INV091	INV099	INV100
Benzylpenicillin	R	R	R	R	R	R	R	R	S	R	R	R	S	R
Ampicillin	R	R	R	R	R	R	R	R	S	R	R	R	S	R
Ocaxillin	S	S	R	R	S	S	R	R	S	R	R	S	S	S
Cefoxitin	S	S	R	R	S	S	R	R	S	R	R	S	S	S
Ceftaroline	S	S	S	S	S	S	S	S	S	I	S	S	S	S
Ceftaroline (pneumonia)	S	S	S	S	S	S	S	S	S	R	S	S	S	S
	INV101	INV108	INV109	INV117	INV120	INV130	INV144	INV148	INV162	INV172	INV179	INV195	INV198	INV202
Benzylpenicillin	R	R	R	S	R	R	R	S	R	R	R	R	R	R
Ampicillin	R	R	R	S	R	R	R	S	R	R	R	R	R	R
Ocaxillin	S	S	S	S	S	R	S	S	S	S	R	R	S	R
Cefoxitin	S	S	S	S	S	R	S	S	S	S	R	R	S	R
Ceftaroline	S	S	S	S	S	S	S	S	S	S	S	R	S	S
Ceftaroline (pneumonia)	S	S	S	S	S	S	S	S	S	S	S	R	S	S

Besides the β-lactam antibiotics mentioned above, 17 other antibiotics were tested. Figure 2.3 illustrates the results of the susceptibility testing by colour (red = resistant; yellow = intermediate; green = susceptible). Despite the widespread resistance to β-lactam antibiotics, appropriate antibiotic therapy would have been possible for the collection of isolates studied this work. All isolates tested susceptible for MRSA standard therapies vancomycin, linezolid and tigecycline. However, isolate INV075 tested resistant to ceftaroline in pneumonia (and intermediate for indications other than pneumonia) and INV195 tested resistant to ceftaroline. Test results of every single isolate are shown in the Annex, Tables 6.1 and 6.2.

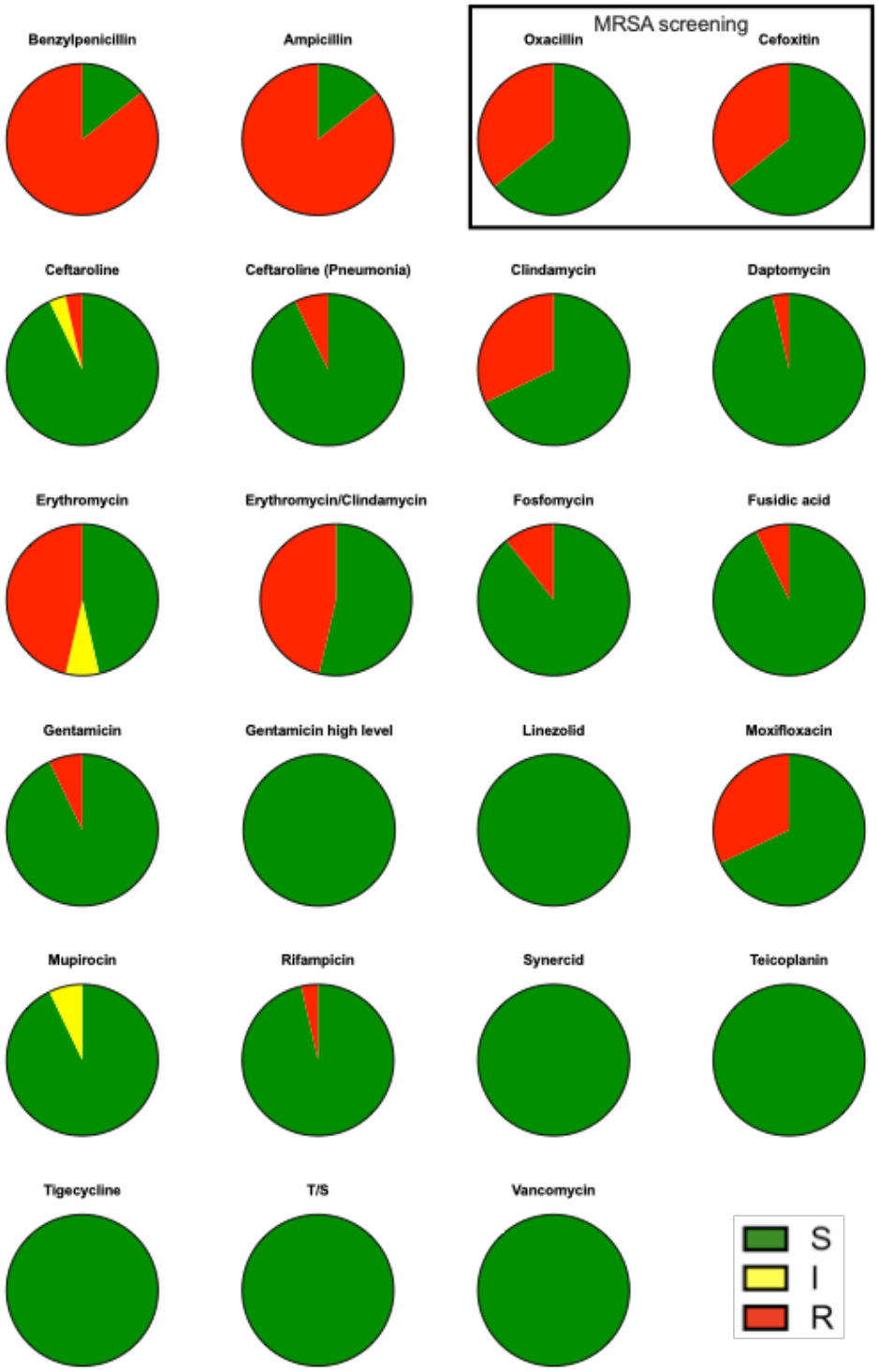

Figure 2.3: Pie charts illustrating the results of the antibiotic susceptibility testing. Each pie chart includes the results of all 28 tested isolates. T/S = trimethroprim/sulfamethoxazole. R = resistant; I = intermediate; S = susceptible.

2.1.4 Multilocus sequence typing of the 30 *S. aureus* isolates

S. aureus is a pathogen with worldwide prevalence. A common way of determining its population biology and answering epidemiological questions is multilocus sequence typing (MLST). The DNA sequences of fragments (402 to 516 bp) of seven housekeeping genes (*arc*, *aroE*, *glpF*, *gmk*, *pta*, *tpi*, *yqiL*) are being compared and define a unique strain type (ST). Every single base difference in a fragment defines a different allele. The combined allelic profile of the seven genes defines the strain type. Isolates with the same sequence in all seven genes are defined as the same strain type. Isolates that share at least five identical alleles, are defined as the same clonal complex (CC) (Chambers & DeLeo, 2009; Enright et al., 2000).

Table 2.7 provides multilocus sequence typing data of the 30 *S. aureus* isolates, generating a broader understanding of the diversity of the isolates. Sequencing was performed according to the original publication (Enright et al., 2000) and is not further described at this point. Represented in the collection of this work were 16 different strain types and six clonal complexes. CC5 was the most prevalent clonal complex (nine isolates), followed by four isolates belonging to CC30, three isolates each to CC8, CC15, and CC45 and two isolates to CC15. The MLST profiles of six isolates were associated with a strain type, but not a clonal complex, and one isolate (INV091) was unable to be assigned a strain type, although it was predicted to be a member of CC30.

Table 2.7: MLST of the 30 *S. aureus* isolates of this work**.** [1]single nucleotide discrepancy present in sequence *(*210T>C); [2]single nucleotide discrepancy present in sequence (114C->T); [3] single nucleotide discrepancy present in sequence (398T>C); *no strain type match for allele pattern (discrepant allele: tpi); SLV = single locus variant.

Isolate	Clonal Complex	Strain Type	*arcC*	*aroE*	*glpF*	*gmk*	*pta*	*tpi*	*yqiL*
CF014	CC30	30	2	2	2	2	6	3	2
CF018	CC45	45	10	14	8	6	10	3	2
CF031	CC8	8	3	3	1	1	4	4	3
CF173	CC5	225 SLV	1	4[1]	1	4	12	25	10
FB02	CC45	45	10	14	8	6	10	3	2
FB04	CC22	737 SLV	7	6[2]	1	70	8	8	6
INV001	CC5	225	1	4	1	4	12	25	10
INV005	CC5	225	1	4	1	4	12	25	10
INV058	---	101	3	1	14	15	11	19	3
INV075	CC5	2112	1	1	1	4	12	1	10
INV078	CC5	225	1	4	1	4	12	25	10
INV091	CC30	*	8	4	2	2	6	181	2
INV099	---	2815	16	410	12	2	13	13	15
INV100	CC5	6	12	4	1	4	12	1	3
INV101	CC22	22	7	6	1	5	8	8	6
INV108	CC15	15	13	13	1	1	12	11	13
INV109	CC15	15	13	13	1	1	12	11	13
INV117	---	101 SLV	3	1[3]	14	15	11	19	3
INV120	CC15	582	13	13	1	1	12	10	13
INV130	CC5	225	1	4	1	4	12	25	10
INV144	CC30	30	2	2	2	2	6	3	2
INV148	---	59	19	23	15	2	19	20	15
INV162	CC45	45	10	14	8	6	10	3	2
INV172	CC30	30	2	2	2	2	6	3	2
INV179	---	80	1	3	1	14	11	51	10
INV195	CC5	5	1	4	1	4	12	1	10
INV198	---	59	19	23	15	2	19	20	15
INV202	CC8	8	3	3	1	1	4	4	3
SA113	CC5	105	1	4	1	4	12	1	28
USA300	CC8	8	3	3	1	1	4	4	3

2.2 Growth of bacterial isolates for RT-PCR and HEK293 cell stimulation

A bead out of the Cryotube stock was streaked out on a TSB agar plate (CASO Agar, pH 7.3 ± 0.2, Carl Roth GmbH + Co. KG, Karlsruhe, Germany) and incubated overnight at 37 °C. The next day, a single colony was picked and inoculated into a 5 mL TSB (Merck KGaA, Darmstadt, Germany) liquid culture (in a 50 mL Erlenmeyer flask) and incubated for 24 hours with shaking at 130 rpm at 37 °C. After 24 hours, cultures were diluted 1:200 (150 µL of previous culture in a new 30 mL liquid culture in a 300 mL Erlenmeyer flask) in either TSB, TSB at pH 5.5, TSB containing 1 M NaCl or TSB with 100 µg/mL ampicillin (Ampicillin sodium salt, Sigma-Aldrich, St. Louis, USA). Cultures were incubated with shaking at 130 rpm for 18 hours at 37°C. After 18 hours, bacterial cells were harvested for RNA-Isolation and HEK293 cell stimulation.

2.3 Gene expression assay (RT-PCR)

RT-PCR is one of the main techniques used to compare the expression of genes. Increased transcription of a gene results in increased mRNA levels over the control condition. This mRNA is transcribed into cDNA by a reverse transcriptase. That is where the “reverse-transcript” within RT-PCR derives from. PCR is a technique to amplify certain genes. In RT-PCR, the amount of amplified DNA is quantified by measuring a fluorescent signal after every PCR amplification cycle. The DNA-dye used in this work was SYBR-Green (LightCycler® 480 SYBR Green I Master, Roche Holding AG, Basel, Switzerland). SYBR-Green is an intercalating dye. It becomes fluorescent by binding double-stranded DNA. That means the dye is not specific to the product of interest but would bind any DNA side-product or primer-dimers. Since primers bind specifically to the gene of interest, all the amplified DNA should derive from the cDNA of interest. This, of course, implies a careful design of the primers. There are two easy ways to make sure only one product was amplified. First, the melting curve of the reaction should only have one specific peak. Second, running the reaction product on a gel should only result in one band (with the size defined by the primers). Figure 2.4 shows the characteristic melting curve peaks of the genes of this work.

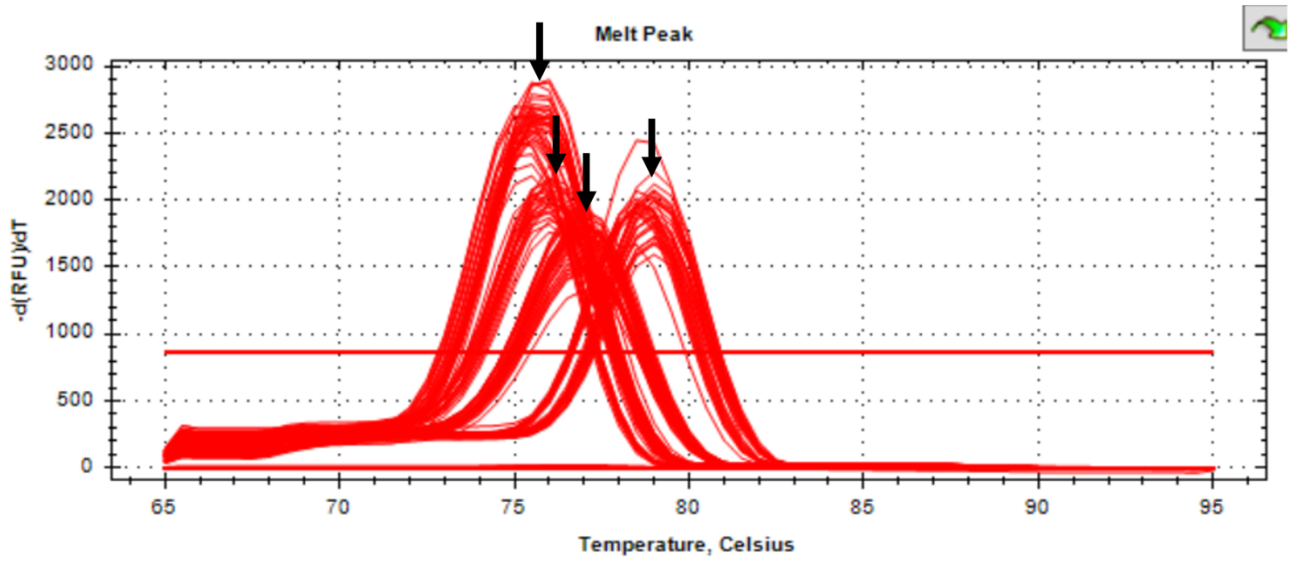

Figure 2.4: Exemplary melting curves after an RT-PCR run on a 384-well plate. The four different PCR products show different melting temperatures. The four peaks, indicated by arrows, belong to amplified gene products of, from left to right, *lnsB*, *geh*, *lnsA* and *rho*. RFU = relative fluorescence units.

Assuming that target-specific amplification and detected fluorescent signal increase correlate, the more cDNA a sample initially contained, the fewer PCR cycles are necessary to detect the signal. When the detected signal exceeds a set threshold, the number of run cycles at this time point defines the sample's C_T value.

A single C_T value is not sufficient by itself. For example, a low C_T value may occur for two different reasons. First, the gene of interest may have been strongly expressed and a lot of cDNA of this gene is present in the sample. Second, there may be generally high amounts of cDNA available in the sample resulting in consequently high amounts of cDNA of the gene of interest. To discriminate between these possibilities, the C_T value of a gene of interest always needs to be compared to the C_T value of a housekeeping gene. A housekeeping gene is constantly expressed in similar amounts and therefore lets one draw quantitative conclusions about genes when comparing its expression to the one of the gene of interest. Initially, while setting up the RT-PCR experiments, *S. aureus 16S* RNA was used as a housekeeping gene. However, it showed very small C_T values, while the genes of interest showed much higher C_T values, as shown in Figure 2.5. These small C_T values could have

complicated calculations. Furthermore, it could not be ruled out that the *16S* C_T values shifted even lower in other isolates, not tested in the PCR test runs.

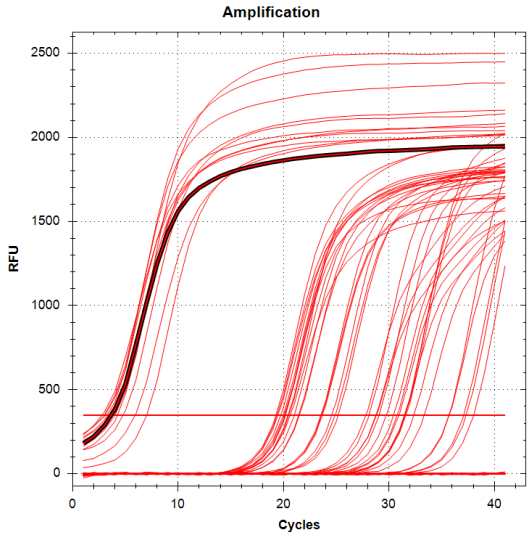

Figure 2.5: RT-PCR amplification curves of *16S* on the left and *lnsA*, *lnsB* and *geh* on the right. RFU = relative fluorescence units.

Thus, the housekeeping gene *16S* was replaced by *S. aureus* gene *rho*. Figure 2.6 shows amplification curves of *rho*, *lnsA*, *lnsB* and *geh* all clearly far away from zero cycles on the x-axis. Thus, all RT-PCR results in this work were performed with *rho* as housekeeping gene.

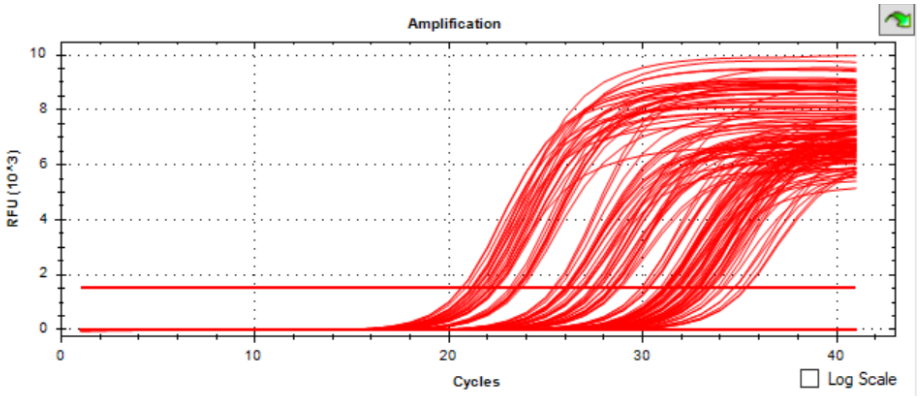

Figure 2.6: RT-PCR amplification curves of *rho*, *lnsA*, *lnsB* and *geh*. RFU = relative fluorescence units.

Several techniques exist to compare the expression of different genes or genes under different conditions. The $2^{-\Delta\Delta CT}$ analysis method was used for RT-PCR analysis in this work. It creates a relative expression level of a treated sample (in this work bacteria grown in low pH, high salt concentrations or in the presence of ampicillin) compared to a control sample (in this work bacteria grown in regular TSB).

One sample was always represented by a technical triplicate, creating 3 C_T values. The mean of those 3 C_T values was calculated:

$C_{T\ mean} = (C_{T1} + C_{T2} + C_{T3}) / 3$

Next, to exclude errors within the cDNA loading of a sample, the $C_{T\ mean}$ of the housekeeping gene was subtracted from the $C_{T\ mean}$ of the gene of interest:

$\Delta C_T = C_{T\ mean,\ gene\ of\ interest} - C_{T\ mean,\ housekeeping\ gene}$

Next, the Δ of the control sample was subtracted from the Δ of the treated sample:

$\Delta\Delta C_T = \Delta C_{T\ treated} - \Delta C_{T\ control}$

Finally, the relative expression of the treated sample compared to the control sample was calculated by using $\Delta\Delta C_T$ as the negative exponent of 2:

relative gene expression = $2^{-\Delta\Delta CT}$

(VanGuilder et al., 2008)

2.3.1 Isolation of *S. aureus* RNA

In order to quantify *S. aureus* gene expression, RNA was isolated and RT-PCR was performed.

2 mL of liquid bacterial culture were centrifuged in a 1.5 mL Micro Tube at 14000 rcf for 3 minutes at room temperature to collect a sufficient amount of bacterial cells. The supernatant was discarded and pelleted bacterial cells were resuspended in 1 mL of TRIzol Reagent (Ambion by life technologies, Carlsbad, USA) and transferred into BashingBead Lysis Tubes

(ZR BashingBead™ Lysis Tubes 0.1 & 0.5 mm Beads, Zymo Research, Freiburg, Germany). In order to extract RNA, the cell wall was disrupted by the Precellys 24 Tissue homogenizer (Bertin Technologies SAS, Montigny-le-Bretonneux, France) (6000 rpm for 40 seconds followed by 3 minutes on ice, again 6000 rpm for 40 seconds, followed again by 3 minutes on ice). Afterwards, the tube was centrifuged at 14000 rcf for 3 minutes at room temperature and the supernatant above the glass beads (containing RNA) was transferred into a DNA LowBinding 1.5 mL Micro Tube and stored at -80°C.

The following steps were performed under a chemical hood:

Frozen samples were thawed for 15 minutes at room temperature. 200 µL Trichlormethan/Chloroform (Carl Roth GmbH + Co. KG, Karlsruhe, Germany) were added and mixed thoroughly by carefully inverting the tube 25 times. The tube was incubated for 3 minutes at room temperature and afterwards centrifuged for 15 minutes at 12000 rcf at 4 °C. Only 200 µL (to prevent contamination with DNA) of the upper (aqueous) phase were transferred into a new 1.5 mL DNA LowBinding Tube. 500 µL 2-Propanol (Sigma-Aldrich, St. Louis, USA) were added and mixed thoroughly by carefully inverting the tube 25 times, followed by 10 minutes incubation at room temperature and 10 minutes in the centrifuge at 12000 rcf at 4 °C. The supernatant was removed carefully and discarded.

The following steps were performed at a specific RNA-bench to avoid DNA contamination and RNA destruction. The workspace and all instruments were cleaned with RNase-ExitusPlus (AppliChem GmbH, Darmstadt, Germany) to minimize unspecific RNAse activity.

1000 µL of 75 % ethanol (Merck KGaA, Darmstadt, Germany) were added to the pellet and carefully mixed by pipetting. The tube was centrifuged for 5 minutes at 7500 rcf at 4 °C. After removing the supernatant carefully without disturbing the pellet, the tube was turned upside down in order to get rid of leftover ethanol. After 15 minutes, the pellet was resuspended in 20 µL of nuclease free water (UltraPure Distilled Water DNase/RNase Free, Invitrogen, Waltham, USA) and left on ice for 15 minutes to fully dissolve.

The RNA content was measured using the NanoDrop One/One (Thermo Fisher Scientific, Massachusetts, USA) as well as the Quantus Fluorometer (Promega GmbH, Walldorf, Germany).

2.3.2 DNase-digest

Deoxyribonucleases are enzymes that degrade DNA, a process that can be helpful to purify RNA samples that are contaminated with DNA. To eliminate leftover genomic DNA within the RNA samples, all samples were digested with DNase I (New England Biolabs, Ipswich, England). The following reaction mix was set up in a 1.5 mL DNA LowBinding Tube on ice: 10 µg RNA, 10 µL DNase I Reaction Buffer (10X), 1 µL DNase I, nuclease free water (UltraPure Distilled Water DNase/RNase Free, Invitrogen, Waltham, USA) (added up to 100 µL). The reaction mix was incubated for 10 minutes at 37 °C, allowing the enzyme to degrade contaminating DNA. Heat-inactivation was performed for 10 minutes at 75 °C to inactivate the DNase activity. Because the amount of genomic DNA in the samples was very high, a second DNase digest was performed on the previously digested samples. In the second digest, 5 µL of the pre-digested RNA sample, 5 µL DNase I Reaction Buffer (10X), 1 µL DNase I and 39 µL nuclease free water were mixed, incubated for 10 minutes at 37 °C and heat-inactivated for 10 minutes at 75 °C.

2.3.3 cDNA synthesis

To perform RT-PCR, the isolated RNA needed to be transcribed into cDNA by the enzyme reverse transcriptase. The enzyme therefore is an RNA-dependent DNA polymerase. cDNA synthesis was performed using the Maxima First Strand cDNA Synthesis Kit for RT-qPCR, with dsDNase (Thermo Fisher Scientific, Massachusetts, USA).

Although all samples had already been digested with a DNase twice, a third digest was performed since it was part of the enzyme kit protocol. The reaction mix included: 8 µL RNA sample (previously digested twice), 1 µL dsDNase Buffer (10X) and 1 µL dsDNase. The reaction was set up in a 1.5 mL DNA LowBinding Tube on ice. After incubation for 10 minutes at 37 °C, 4 µL Reaction Mix (5X), 2 µL Maxima Enzyme Mix and 4 µL nuclease free water (UltraPure Distilled Water DNase/RNase Free, Invitrogen, Waltham, USA) were added and

incubated for 10 minutes at 25 °C, followed by 30 minutes at 50 °C. For heat-inactivation the temperature of the heating block was increased to 85°C for 13 minutes. The temperature increased quite slowly, so the actual time at 85 °C was only 5 minutes. Afterwards, tubes were stored at -80 °C.

At this point, two types of controls had to be produced for the following RT-PCR. Firstly, the “reverse transcriptase negative control”, that contained all reagents mentioned above except the Maxima Enzyme Mix. This control ensured that the samples were not contaminated with genomic DNA. It had to be done for every RNA sample. Secondly, the “no template control”, that contained all reagents except the RNA sample. This control ensured that the reagents or the workspace were not contaminated. This control was done once per cDNA synthesis process (which included multiple RNA samples).

2.3.4 RT-PCR

RT-PCR was performed on either a 96- or a 384-well plate, always working with 10 µL reactions. Primers are listed in Table 2.8, the PCR reaction mix in Table 2.9. The PCR workspace was continuously cleaned with ROTI Nukleinsäurefrei (Carl Roth GmbH + Co. KG, Karlsruhe, Germany) to avoid DNA contamination.

Table 2.8: Primers used for RT-PCR in this work

Gene	Primer Sequence
rho	GTTTTACCTGCTTTAGGTGGCG
	AAACGTCCGCATTTCCAAGC
lnsA	ACTCACCAAAAACAATTGCAGATA
	TACAAATTGAGGGGCCTGGC
lnsB	ACGTGATATTGGATTTATTTTCCTT
	CTGCGAGTAAATAGCTAATGTTCA
geh	AGCAGCTGATAAGTTTGGAAATACA
	GTCCAAATTTTGCTTTTACTAACGC

Table 2.9: RT-PCR reaction mix per well

Reagent	**Volume (µL) for 10 µL reaction**
sample (cDNA, diluted 1:5)	1
primer forward (diluted 1:10, final reaction concentration 300 nM)	0.3
primer reverse (diluted 1:10, final reaction concentration 300 nM)	0.3
LightCycler® 480 SYBR Green I Master Mix (containing the DNA polymerase and the DNA dye)	5
UltraPure™ Distilled Water DNase/RNase Free (Invitrogen, Waltham, USA)	3.4

RT-PCR was performed as described in Table 2.10 using the CFX96 Touch Real-Time PCR Detection System and CFX384 Touch Real-Time PCR Detection System with C1000 Touch Thermal Cycler and the corresponding analysis software CFX Maestro (Bio-Rad Laboratories, Inc., Hercules, California, USA).

Table 2.10: RT-PCR program. The lid temperature was at 105 °C.

PCR step	**Temperature (°C)**	**Time (s)**	**Repeats**
Initial Denaturation	95	300	1
Denaturation	95	10	40
	decrease by 4.4 °C per second		
Annealing	57	20	
	increase by 2.2 °C per second		
Extension	72	15	
Plate read			
	increase by 4.4 °C per second		
Final Extension	65	5	1
	increase from 65 °C to 95 °C in 0.5 °C per 5 seconds		
Plate read			1
End	25	infinite hold	1

2.4 HEK293 cell Toll-like receptor stimulation assay

2.4.1 Growth of HEK293 cells

HEK293 cells (American Type Culture Collection ATCC, Virginia, USA) were grown in DMEM (+ 10 % FBS + 1 % penicillin/streptomycin + 1 % L-glutamine) in 75 cm^2 flasks at 37 °C with 5 % CO_2. Manufacturers are listed in Table 2.11. As the cells were attached to the flask, the media could be aspirated without losing cells and the flasks were washed with 10 mL PBS to get rid of unattached cells. The PBS, including unattached HEK293 cells, was aspirated. 10 mL of 2mM EDTA solution were added to each flask and incubated for 5 minutes at 37 °C to detach the attached cells. Cell clusters were loosened by pipetting up and down twice with a 10 mL pipet. Suspended HEK293 cells were centrifuged in a 50 mL reaction tube for 6 minutes at 360 rcf at room temperature. The supernatant was discarded and pelleted cells were washed by resuspending them in 10 mL PBS and spinning them back down for 6 minutes at 360 rcf at room temperature. Pelleted cells were resuspended in 10 mL DMEM (+ 10 % FBS + 1 % penicillin/streptomycin + 1 % L-glutamine) and counted using Trypan Blue Stain (0.4 %) (Gibco, Life Technologies Corporation, New York, USA) and the TC20 Automated Cell Counter (Bio-Rad Laboratories, Inc., Hercules, California, USA).

Table 2.11: Material needed in HEK293 cell culture

Name	**Manufacturer**
DMEM	Gibco, Life Technologies Corporation, New York, USA
EDTA	Paul-Ehrlich-Institute, Langen, Germany
Fetal Bovine Serum (FBS)	Sigma-Aldrich, St. Louis, USA
L-Glutamine 200 mM (100X)	Gibco, Life Technologies Corporation, New York, USA
PBS without Ca and Mg (pH 7.1)	Paul-Ehrlich-Institut, Langen, Germany
Penicillin-Streptomycin	Gibco, Life Technologies Corporation, New York, USA

2.4.2 Preparation of *S. aureus* protein lysates as stimuli

12 mL of bacterial liquid culture were transferred into a 50 mL centrifuge tube and centrifuged at 4700 rcf for 10 minutes at 4 °C. The supernatant was discarded and pelleted bacterial cells were resuspended in 2 mL of TSB. 1 mL was transferred into a 1.5 mL tube and centrifuged

at 14000 rcf for 3 minutes at room temperature. The supernatant was discarded and the pellet stored at -20 °C for later use. After thawing the pellet, bacterial cells were resuspended in 500 µL of RIPA buffer (SERVA Electrophoresis GmbH, Heidelberg, Germany). 5 µL protease-inhibitor (Halt Protease Inhibitor Cocktail (100X), Thermo Fisher Scientific, Massachusetts, USA) were added and the suspension transferred into into BashingBead Lysis Tubes. Bacterial cells were disrupted by the Precellys 24 Tissue homogenizer (6000 rpm for 40 seconds followed by 3 minutes on ice, again 6000 rpm for 40 seconds, followed again by 3 minutes on ice). Afterwards, the tube was centrifuged at 14000 rcf for 3 minutes at room temperature and the bacterial lysate above the glass beads was transferred into a protein LowBinding 1.5 mL Micro Tube and stored at -20°C.

The protein concentration of the lysates was measured by Pierce Protein BCA Assay (Thermo Fisher Scientific, Massachusetts, USA). The working reagent of the kit reacts with proteins and leads to colorimetric detection. Since an approximately linear relationship exists between the colour intensity and protein concentration, OD_{550} readings can be used for quantitative protein calculations. Protein lysates were diluted 1:20 in PBS, and 20 µL of the dilution were added to 180 µL working reagent and incubated for 30 minutes at 37 °C. The same incubation time was performed for a standard with a known protein concentration. Absorbance was measured at 550 nm wavelength using the Sunrise absorbance reader (Tecan, Männedorf, Switzerland). Knowing the protein concentrations of the standard dilution, the absorbance of those wells could be used to interpolate a standard curve (line) taking the protein concentrations as x-values and the measured absorbances as y-values. Given the interpolated standard curve, each lysate-absorbance could be used to calculate a protein concentration. This process is described in further detail in chapter 2.4.5 (IL-8-ELISA).

2.4.3 Transient Transfection of HEK293 cells

Transient transfection is a method to express plasmid-encoded genes for a limited time in eukaryotic cells. The transfected DNA enters the nucleus and is transcribed. The plasmid DNA is, as opposed to stable transfection, not incorporated into the genomic DNA. The human cells transfected in this work were human embryonic kidney 293 cells (HEK293 cells). HEK293 cells are a commonly used cell line in scientific research as well as pharmaceutical

manufacturing. They show a high transfection efficiency as well as all human posttranslational modifications (Hu et al., 2018).

50 000 HEK293 cells were seeded per well in 100 µL DMEM (+ 10 % FBS + 1 % penicillin/streptomycin + 1 % L-glutamine) on a 96-well flat bottom plate and incubated for 24 hours at 37 °C with 5 % CO_2 prior to assay. Since *S. aureus* isolates were grown in four different conditions and stimulations were performed in triplicates, 16 wells were needed per *S. aureus* isolate per plasmid. Since three plasmids were used and the stimulation was performed in untransfected HEK293 cells as a negative control as well, 64 wells were needed in total per *S. aureus* isolate (Figure 2.7).

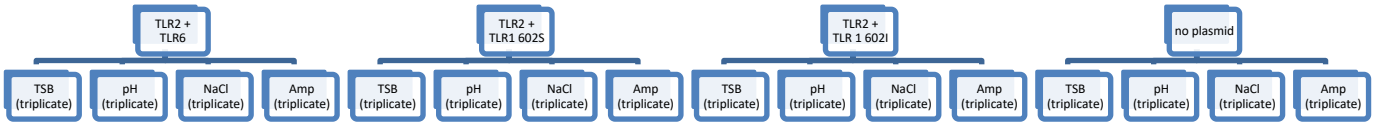

Figure 2.7: Overview of the 64 stimulations performed with each *S. aureus* isolate. The stimulated cells included HEK293 cells expressing either TLR2 + TLR6, TLR2 + TLR1 602S, TLR2 + TLR1 602I or no TLRs at all. The stimuli included bacteria grown in regular TSB, in low pH, high salt concentrations and in the presence of ampicillin.

After 24 hours, cells had a confluency of 60 - 70 %. Three different plasmids were used in this work for transient transfection (Table 2.12). All plasmids encoded human TLR2 and one additional human TLR (either TLR6, TLR1 602S or TLR1 602I). The old media was aspirated from each well. 0.25 µL lipofectamine (Lipofectamine 2000, Invitrogen, Waltham, USA) and 100 ng plasmid DNA were added to each well and the volume was filled up to 50 µL with Opti-MEM (Gibco, Life Technologies Corporation, New York, USA). Two types of negative controls were performed in this experiment. First, the lipofectamine control containing all reagents mentioned above except for plasmid DNA (0.25 µL lipofectamine, 49.75 µL OptiMEM). Second, the no plasmid control in which only 50 µL OptiMEM were added to the HEK293 cells. Besides the varying reagents, all negative controls and transfected cells were treated the same way. Plates were centrifuged for 6 minutes at 360 rcf at room temperature

and incubated for 2 hours at 37 °C with 5 % CO_2. 50 µL of OptiMEM were added per well and the plates incubated for 20 hours at 37 °C with 5 % CO_2. After 20 h, cells had a confluency of 70 - 80 %. In this experimental setup, transfected blasticidin resistance was not made use of.

Table 2.12: Plasmids used for transient transfection of HEK293 cells

Plasmid	Genes cloned	Resistence-Gene	Source	Stock
pDUO-hTLR6/TLR2	Human TLR6 and TLR2	Blasticidin	InvivoGen, Toulouse, France	30 ng / µL
plD043	Human TLR2 and TLR1 602S	Blasticidin	InvivoGen, Toulouse, France; mutated by Dr. Karen Huber, Paul-Ehrlich-Institut, Langen, Germany	114 ng / µL
plD044	Human TLR2 and TLR1 602I	Blasticidin	InvivoGen, Toulouse, France; mutated by Dr. Karen Huber, Paul-Ehrlich-Institut, Langen, Germany	179 ng / µL

2.4.4 Stimulation of transfected HEK293 cells

The 50 µL (lipofectamine, plasmid DNA and optiMEM) were aspirated and 90 µL of DMEM (+ 10 % FBS + 1 % penicillin/streptomycin + 1 % L-glutamine) were added to each well. Furthermore, 10 µL of the protein lysates (concentration 200 ng / mL) were added to each well and cells were incubated for 20 hours at 37 °C with 5 % CO_2. After 20 hours, the confluency was at almost 100% in every well. There were neither unusual clusters of cells, nor a lot of dead cells or contamination. Plates were centrifuged for 6 minutes at 360 rcf at room temperature and 80 µL of the supernatant (including the secreted IL-8) were transferred onto a new 96-well plate. The plate was sealed and stored at -20 °C until used for IL-8-ELISA (at least overnight). Besides stimulating cells with protein lysates, cells were stimulated with synthetic lipoprotein ligands and treated the same way. Those ligands included Pam-Dhc-SKKKK (Pam_1CSK_4), Pam_2Cys-SKKKK (Pam_2CSK_4) and Pam_3Cys-SKKKK (Pam_3CSK_4) (all

EMC microcollections GmbH, Tübingen, Germany). Stimulations with these synthetic ligands were performed using a concentration of 100 ng/mL.

2.4.5 IL-8-ELISA

Enzyme-linked immunosorbent assay (ELISA) is a broadly used technique to quantify proteins. Different ELISA protocols have been developed over time. The method used in this work was the Antibody-sandwich ELISA: An antibody (capture antibody) against the protein to be quantified (antigen) gets attached to a microtiter plate. Next, the sample containing the antigen is added to the well, enabling the antigen to bind to the capture antibody. To visualize the amount of bound antigen, a second antibody (detection antibody) against the antigen is added. The detection antibody is conjugated with an enzyme. An added substrate gets hydrolyzed and becomes fluorescent. The created fluorescent signal intensity is proportional to the amount of protein in the sample. All incubation steps are time sensitive and between every incubation step, wells need to be washed to remove all soluble, unbound reagents (Hornbeck, 2015). Figure 2.8 illustrates all mentioned working steps.

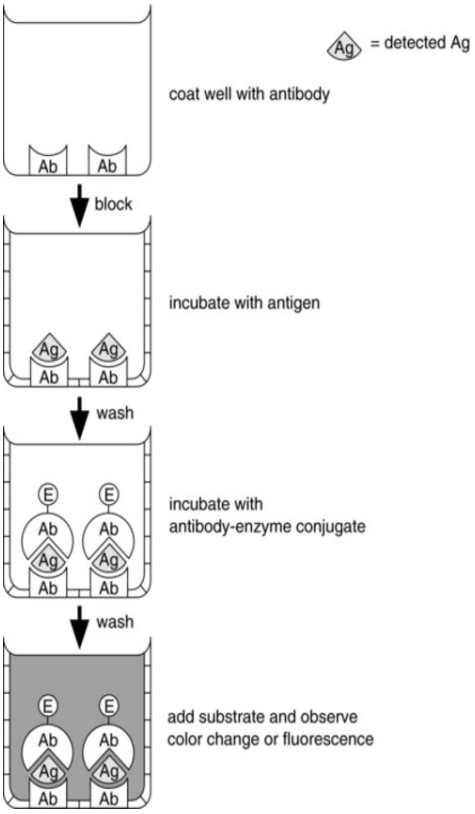

Figure 2.8: Working steps in Antibody-sandwich ELISA top down. CP in Immunology, Volume: 110, Issue: 1, Pages: 2.1.1-2.1.23, First published: 03 August 2015, DOI: (10.1002/0471142735.im0201s110) (Hornbeck, 2015)

ELISAs in this work were performed using the Human IL-8 ELISA Set (BD Biosciences Pharmingen, San Diego, USA). The antigen to be quantified in this work was soluble human IL-8. The capture antibody was an anti-human IL-8 monoclonal antibody. The detection antibody was a biotinylated anti-human IL-8 monoclonal antibody. The enzyme was Streptavidin-horseradish peroxidase conjugate (SAv-HRP). All reagents are listed in Table 2.13 with the corresponding chemicals in Table 2.14.

96-well plates (half-area) were coated with 50 µL of capture antibody (1:500 dilution in coating buffer) per well and incubated overnight at 4 °C. Wells were aspirated and washed 3 times with 150 µL of wash buffer, blocked with 150 µL of assay diluent and incubated at room temperature for 1 hour. Wells were aspirated and washed 3 times with 150 µL of wash buffer. A serial dilution of recombinant human IL-8-standard was put on the plates in duplicates

(involving 200, 100, 50, 25, 12.5, 6.25, 3.125 and 0 pg/mL). 50 µL of sample (1:10 diluted in assay diluent) were added to each well and incubated for two hours at room temperature. Wells were aspirated and washed 5 times with 150 µL of wash buffer. 50 µL of detection antibody and enzyme reagent (1:500 dilution in assay diluent) were added to each well and incubated for 1 hour at room temperature. Wells were aspirated and washed 7 times with 150 µL of wash buffer. 50 µL of substrate solution were added to each well and incubated for 30 minutes at room temperature in the dark. 25 µL of stop solution were added to each well and the absorbance was measured at 450 nm with the Sunrise absorbance reader (Tecan, Männedorf, Switzerland) and its recommended software Magellan 2.0 (Tecan, Männedorf, Switzerland). Plates were sealed for all incubation times except the incubation of the stop solution. All washing steps were performed using the HydroFlex Plus microplate washer (Tecan, Männedorf, Switzerland).

Table 2.13: Buffers and solutions used in IL-8 ELISA

ELISA Reagent	**Composition**
assay diluent	PBS with 10 % FBS
coating buffer	0.1 M Sodium Carbonate, pH 9.5, 7.13 g $NaHCO_3$, 1.59 g Na_2CO_3, q.s. to 1.0 L; pH to 9.5 with 10 N NaOH.
stop solution	2 N H_2SO_4
substrate solution	TMB and H_2O_2
wash buffer	PBS with 0.05 % Tween 20

Table 2.14: Chemicals needed for buffers and solution in IL-8-ELISA

Chemical	**Manufacturer**
BD OptEIA TMB Substrate Reagent Set	BD Biosciences Pharmingen, San Diego, USA
hydrogen peroxide 30%	Merck KGaA, Darmstadt, Germany
sodium carbonate	Merck KGaA, Darmstadt, Germany
sodium hydrogen carbonate	Merck KGaA, Darmstadt, Germany
Sodium Hydroxide 10 mol/l (10 N)	AppliChem GmbH, Darmstadt, Germany
sulfuric acid	Sigma-Aldrich, St. Louis, USA
Tween 20	Carl Roth GmbH + Co. KG, Karlsruhe, Germany

Knowing the IL-8 concentration of the standard-dilution, the absorbance of those wells could be used to interpolate a standard curve (line) taking the IL-8 concentrations as x-values and the measured absorbance as y-values (Figure 2.9). The absorbances of the samples could now be used to calculate IL-8 concentrations. Since the samples were diluted 1:10, the calculated concentration needed to be multiplied by 10.

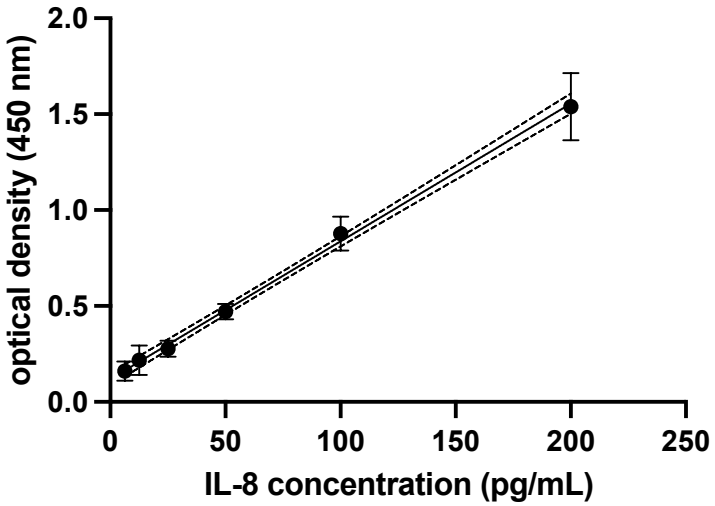

Figure 2.9: Interpolated standard curve of IL-8 standards

2.5 Sanger sequencing of genes of interest

Different sequencing techniques have developed over time. In this work, genes were sequenced by Sanger sequencing. Sanger sequencing functions similar to PCR amplification, with the difference of additional chain-terminating dideoxynucleotide triphosphates (ddNTPs). To analyze one DNA sequence, four different PCR reactions are needed. Every reaction consists of DNA, a polymerase, the 4 deoxynucleotide triphosphates (dNTPs) and one of four ddNTPs. For example, the reaction mix to determine adenine consists of all dNTPs plus ddATP. Thus, after many PCR cycles, a lot of different length products are amplified always ending at the position of adenine. Therefore, sorting the DNA amplicons of the 4 reactions by size on a gel dictates the amplified sequence. The generation of base-determining peaks in a chromatogram is called “base calling”. Ideally, there is only

one peak at a time suggesting precise sequences. If a distinct assignment of a base is not possible, the base position is defined as “N”. Logically, the higher the “N”- rate in a predicted sequence, the worse the sequencing reliability. The alignment of the forward and reverse sequence is called “sequence assembling”. Ideally those sequences are completely corresponding leading to the consensus sequence. A disadvantage of the method is the poor accuracy at the beginning of the sequence, right after the primer, as well as at the end of a sequence, after around 900 base pairs. Those areas should be excluded from analysis (Crossley et al., 2020).

2.5.1 Growth of bacteria for isolation of genomic DNA

A bead out of the Cryotube stock was streaked out on a TSB agar plate (CASO Agar, pH 7.3 ± 0.2, Carl Roth GmbH + Co. KG, Karlsruhe, Germany) and incubated overnight at 37 °C. The next day, a single colony was picked and inoculated into a 20 mL TSB (Merck KGaA, Darmstadt, Germany) liquid culture and incubated overnight shaking at 130 rpm at 37 °C.

2.5.2 Isolation of genomic *S. aureus* DNA

20 mL of liquid bacterial culture were centrifuged in a 50 mL centrifuge tube at 4700 rcf for 10 minutes at room temperature. The supernatant was discarded and the following reagents added to the bacterial cell pellet: 4 mL buffer P1 (QIAGEN GmbH, Hilden, Germany), 100 µg lysostaphin and 30 mg lysozyme. After a one-hour incubation shaking at 130 rpm at 37 °C, 200 mL of saturated SDS solution were added followed by another incubation for 5 minutes shaking at 130 rpm at 37 °C. 1.3 mL $NaClO_4$ (5M) were added to the tube and vortexed for a few seconds. 6 mL Chloroform:Isoamyl alcohol were added to the tube and incubated for 2 minutes at room temperature. The tube was centrifuged at 5500 rcf for 10 minutes at room temperature. The supernatant (containing the genomic DNA) was carefully transferred into a new 15 mL tube and the volume was measured. The solution was decanted into another 50 mL tube filled with 100 % ice cold ethanol (twice the volume of the decanted DNA solution). The DNA precipitated and was wrapped around an inoculation loop. Attached to the inoculation loop, it was washed twice in 70 % ethanol and finally dissolved in 1 mL nuclease free water. DNA samples were stored at -20 °C. Manufacturers of all reagents are listed in Table 2.15.

Table 2.15: Reagents used for the isolation of *S. aureus* genomic DNA

Name	**Manufacturer**
Buffer P1	QIAGEN GmbH, Hilden, Germany
Chloroform : Isoamylalkohol 24:1	AppliChem GmbH, Darmstadt, Germany
Ethanol	Merck KGaA, Darmstadt, Germany
Lysostaphin from *Staphylococcus staphylolyticus*	Sigma-Aldrich, St. Louis, USA
Lysozyme, from chicken egg white	Sigma-Aldrich, St. Louis, USA
Sodium Dodecyl Sulphate	Merck KGaA, Darmstadt, Germany
Sodium perchlorate monohydrate	Merck KGaA, Darmstadt, Germany
UltraPure Distilled Water DNase/RNase Free	Invitrogen, Waltham, USA

2.5.3 Sample preparation

Sanger sequencing was performed at Eurofins Genomics Europe Pharma and Diagnostics Products & Services Sanger/PCR GmbH. The samples sent off to sequencing can either be isolated DNA or a PCR amplicon. In this work, a PCR product was sent to Sanger sequencing. Consequently, a PCR had to be performed with different primers than those from the RT-PCR experiment since this time the PCR product had to include the entire gene of interest. PCRs were performed with Phusion High-Fidelity DNA-Polymerase, 500 Units, 2 U/µl (Thermo Fisher Scientific, Massachusetts, USA) according to the manufacturer's protocol. Sequencing primers are listed in Table 2.16, the PCR reaction mix in Table 2.17 and the PCR program in Table 2.18.

Table 2.16: Primers used for sequencing purpose

Gene	**Primer Sequence**
lnsA	CTCAATGATGTTTCAGACTGTT
	CCCAATTTATTGCAAAACAAAAAC
lnsB	ACAAAACAAAACACAATGGAAGCG
	ACATGAAACATTCTATATGGCTCGT
lnsB (promoter)	CTCATACCAGATTGTCCTACGATACG
	CTTGTTGAGTGAATACAGCTACTAACCC
	GTAGCGTATTCTTCTTCTATGTAATGTTT
geh	AAGCGCAATTGCACCTACTG
	TCGTAGACCTAATGACGAAGCA
	CGCCATAATCTACGCGACCA
	CTGAACGACAAGGTTCTAAACAGTCACACC

Table 2.17: PCR reaction mix for sequencing purpose

Reagent	**Volume (µL) for 50 µL reaction**
UltraPure Distilled Water DNase/RNase Free (Invitrogen, Waltham, USA)	37
5 X Phusion HF Buffer	10
10 mM dNTPs (Deoxynucleotide Solutions, Mix, New England Biolabs, Ipswich, England)	1
Primer forward	0.25
Primer reverse	0.25
DNA	1
Phusion High-Fidelity DNA Polymerase	0.5

Table 2.18: PCR program for sequencing purpose

Reaction	**Time (s)**	**Temperature (°C)**	**Repeats**
Initial Denaturation	30	98	1
Denaturation	10	98	35
Annealing	30	depending on primers	
Extension	90	72	
Final Extension	600	72	1
Hold	infinite	4	1

All PCR products were run on a 1 % agarose gel to confirm successful amplification (by one homologous band of expected size). Material for agarose gel electrophoresis is listed in Table 2.19.

Table 2.19: Material needed for agarose gel electrophoresis

200 bp DNA Ladder	Jena Bioscience, Jena, Germany
Agarose SERVA Premium	SERVA Electrophoresis GmbH, Heidelberg, Germany
FastRuler High Range DNA Ladder	Thermo Fisher Scientific, Massachusetts, USA
FastRuLer Middle Range DNA Ladder	Thermo Fisher Scientific, Massachusetts, USA
PowerPac Basic Power Supply	Bio-Rad Laboratories, Inc., Hercules, California, USA
Sub-Cell GT Horizontal Electrophoresis System, 15 x 10 cm tray	Bio-Rad Laboratories, Inc., Hercules, California, USA
TAE	Paul-Ehrlich-Institute, Langen, Germany
TriTrack DNA-Ladefarbstoff (6x)	Thermo Fisher Scientific, Massachusetts, USA

The following sequencing reaction mix was set up in a 1.5 mL DNA LowBind Micro tube and sent off to Eurofins Genomics: 3 µL of the 1:10 diluted PCR product, 27 µL nuclease free water (UltraPure Distilled Water DNase/RNase Free, Invitrogen, Waltham, USA), 4 µL of a 1:10 diluted sequencing primer.

2.6 Analysis

Data analysis was performed using Microsoft Office 2023 (Microsoft Corporation, Redmond, USA) and GraphPad Prism 9 (Graphstats, Bangalore, India).

Phylogenetic trees were created using the softwares CodonCode Aligner (CodonCode Corporation, Centerville, MA, USA) and UGENE (Unipro, Novosibirsk, Russia). Protein alignments were created using the MUSCLE algorithm in SnapGene (GSL Biotech LLC, Boston, USA). Promoter sequences were predicted by BPROM (Softberry, Inc., Mount Kisco, USA).

Statistical significances in RT-PCR and ELISA experiments were calculated by Wilcoxon matched-pairs signed rank test. Correlation was calculated using the Spearman correlation.

2.7 Other Materials

Table 2.20: Laboratory devices

Device	Manufacturer
Centrifuge 5418	Eppendorf, Hamburg, Germany
Centrifuge 5424 R	Eppendorf, Hamburg, Germany
Centrifuge 5810 R	Eppendorf, Hamburg, Germany
DensiCHEK™ Plus	bioMérieux, Inc., Durham, North Carolina, USA
Eismaschine	ZIEGRA Eismaschinen GmbH, Isernhagen, Germany
Galaxy 170 S CO_2 Incubator	Eppendorf, Hamburg, Germany
Heraeus B 6200 incubator	Heraeus, Hanau, Germany
Microscope Primovert	Carl Zeiss Microscopy Deutschland GmbH, Oberkochen, Germany
Multifuge X3R Centrifuge	Thermo Fisher Scientific, Massachusetts, USA
New Brunswick Innova 44 Shaker	Eppendorf, Hamburg, Germany
Photometer DEN-600	Biosan, Riga, Lettland
Safe 2020 Class II Biological Safety Cabinet	Thermo Fisher Scientific, Massachusetts, USA
TH21 Heizblockthermostat	HLC BioTech, Bovenden, Germany
Thermoshaker with Cooling for Microtubes and Microplates	Grant Instruments Europe B.V., Amsterdam, The Netherlands
VF2 (vortex mixer)	Janke & Kunkel GmbH & Co. KG
Vibrofix VF1 Electronic	IKA-Werke GmbH & Co. KG, Staufen, Germany

Table 2.21: Pipets

Pipet	Manufacturer
Eppendorf Research plus, 1-channel, 0.1 – 2.5 µL	Eppendorf, Hamburg, Germany
Eppendorf Research plus, 1-channel, 0.5 – 10 µL	Eppendorf, Hamburg, Germany
Eppendorf Research plus, 1-channel, 10 – 100 µL	Eppendorf, Hamburg, Germany
Eppendorf Research plus, 1-channel, 100 – 1000 µL	Eppendorf, Hamburg, Germany
Eppendorf Research plus, 8-channel, 0.5 – 10 µL	Eppendorf, Hamburg, Germany
Eppendorf Research plus, 8-channel, 10 – 100 µL	Eppendorf, Hamburg, Germany
Eppendorf Research plus, 8-channel, 120 – 1200 µL	Eppendorf, Hamburg, Germany
Eppendorf Research plus, 8-channel, 30 – 300 µL	Eppendorf, Hamburg, Germany
PIPETBOY acu 2	INTEGRA Biosciences AG, Zizers, Switzerland
Sartorius eLINE 8-channel 50 - 1200 µl Electronic Pipette	Sartorius AG, Göttingen, Germany

Table 2.22: Disposable plastic ware

Name	Manufacturer
Biosphere Fil. Tip 20 neutral	Sarstedt AG & Co., Nümbrecht, Germany
Cell Culture Flask, 50 mL, 75 cm^2, PS	Greiner Bio-One International GmbH, Kremsmünster, Austria
Cellculture microplate, 96 wells, PS, F-bottom	Greiner Bio-One International GmbH, Kremsmünster, Austria
Cryobank	Mast Group Ltd, Bootle, UK
Cuvettes 10 x 4 x 45 mm	Sarstedt AG & Co., Nümbrecht, Germany
ep T.I.P.S Standard 0.5 – 20 µL	Eppendorf, Hamburg, Germany
ep T.I.P.S Standard 50 - 1000 µL	Eppendorf, Hamburg, Germany
Filter tips 10 µL	BRAND GMBH + CO KG, Wertheim, Germany
Filter tips 100 µL	nerbe plus GmbH & Co. KG, Winsen, Germany
Filter tips 1000 µL	Biofil, Guangzhou, China
Filter tips 200 µL	Biofil, Guangzhou, China
Filter tips 200 µL	nerbe plus GmbH & Co. KG, Winsen, Germany
Filterspitzen AXON 1000 µL	Axon Labortechnik GmbH, Kaiserslautern, Germany
Hard-Shell 384-Well PCR Plates, thin wall, skirted, white/clear	Bio-Rad Laboratories, Inc., Hercules, California, USA
Hard-Shell 96-Well PCR Plates, low profile, thin wall, skirted, white/clear	Bio-Rad Laboratories, Inc., Hercules, California, USA
Inoculation loop 1 µL	Sarstedt AG & Co., Nümbrecht, Germany
Inoculation loop 10 µL	Sarstedt AG & Co., Nümbrecht, Germany
Mic Tubes and Caps	Bio Molecular Systems, Upper Coomera, Australia
Micro tube 1.5 mL DNA LowBind	Sarstedt AG & Co., Nümbrecht, Germany
Micro tube 1.5 mL protein LB	Sarstedt AG & Co., Nümbrecht, Germany
Microplate, 96 Well, PS, Half Area, Clear, Microlon, High Binding,10 PCS/BAG	Greiner Bio-One International GmbH, Kremsmünster, Austria
Pipette tip 200 µl	Sarstedt AG & Co., Nümbrecht, Germany
Pipette, 10 mL	Greiner Bio-One International GmbH, Kremsmünster, Austria
Pipette, 25 mL	Greiner Bio-One International GmbH, Kremsmünster, Austria
Pipette, 5 mL	Greiner Bio-One International GmbH, Kremsmünster, Austria
Pipette, 50 mL	Greiner Bio-One International GmbH, Kremsmünster, Austria

Reaction tube 1.5 mLl, PP	Sarstedt AG & Co., Nümbrecht, Germany
Tube 5 mL, 75x12 mm, PS	Sarstedt AG & Co., Nümbrecht, Germany
Tube, 15 ml, PP, 17/120 MM, conical bottom	Greiner Bio-One International GmbH, Kremsmünster, Austria
Tube, 50 ml, PP, 30/115 MM, conical bottom	Greiner Bio-One International GmbH, Kremsmünster, Austria
Wooden applicator with cotton tip 2.2 x 150 mm	nerbe plus GmbH & Co. KG, Winsen, Germany

3 Results

3.1 Gene Sequencing revealed a more conserved locus for *InsA* than for *InsB*

DNA sequencing of *InsA* and *InsB*, the two genes together sufficient to perform tri-acylation on *S. aureus* lipoproteins, showed differences in the level of their nucleic acid heterogeneity between the two loci. The *InsA* locus was highly conserved within the 30 isolates (Figure 3.1). While isolates sharing the same clonal complex often showed no nucleic acid differences, the differences between different clonal complexes were usually small.

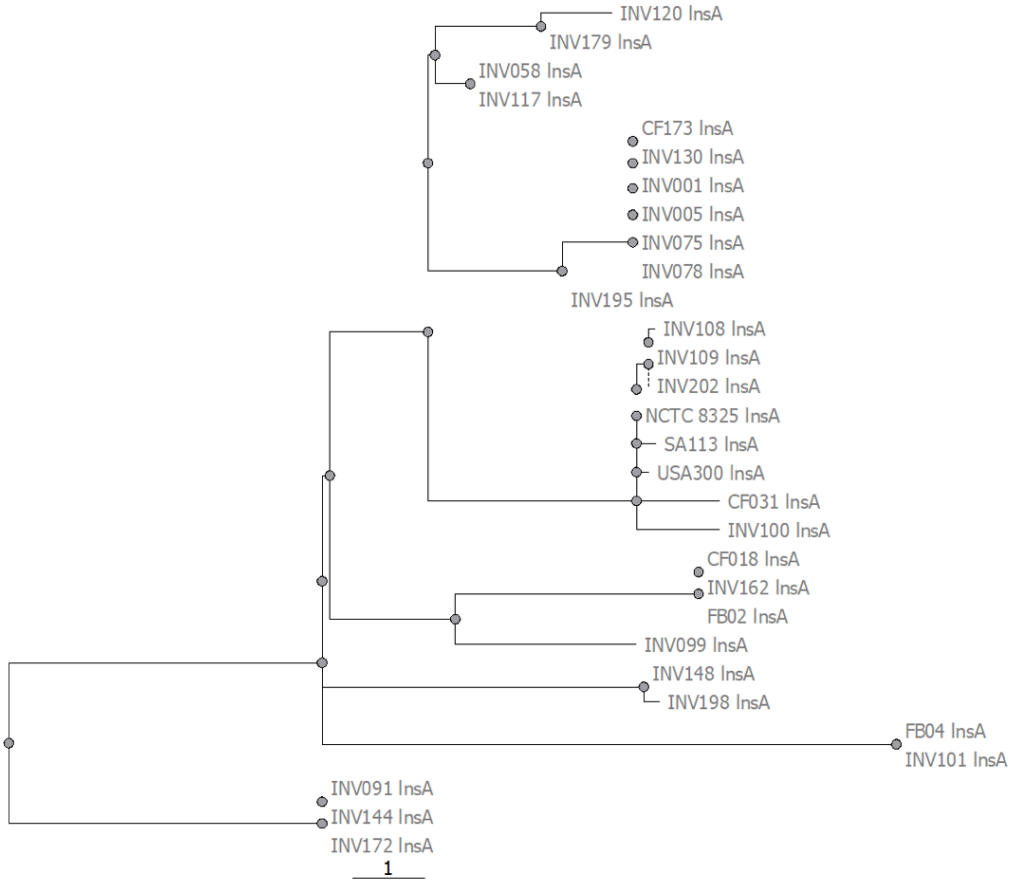

Figure 3.1: Phylogenetic tree of the *InsA* locus. The *InsA* locus of CF014 was unable to be sequenced and is not included in this phylogenetic tree.

Homology increased when translating the *InsA* DNA sequence into amino acid sequence (Figure 3.2). Most of the nucleic acid differences were either silent and resulted in the same amino acid or in substitution with a conserved amino acid.

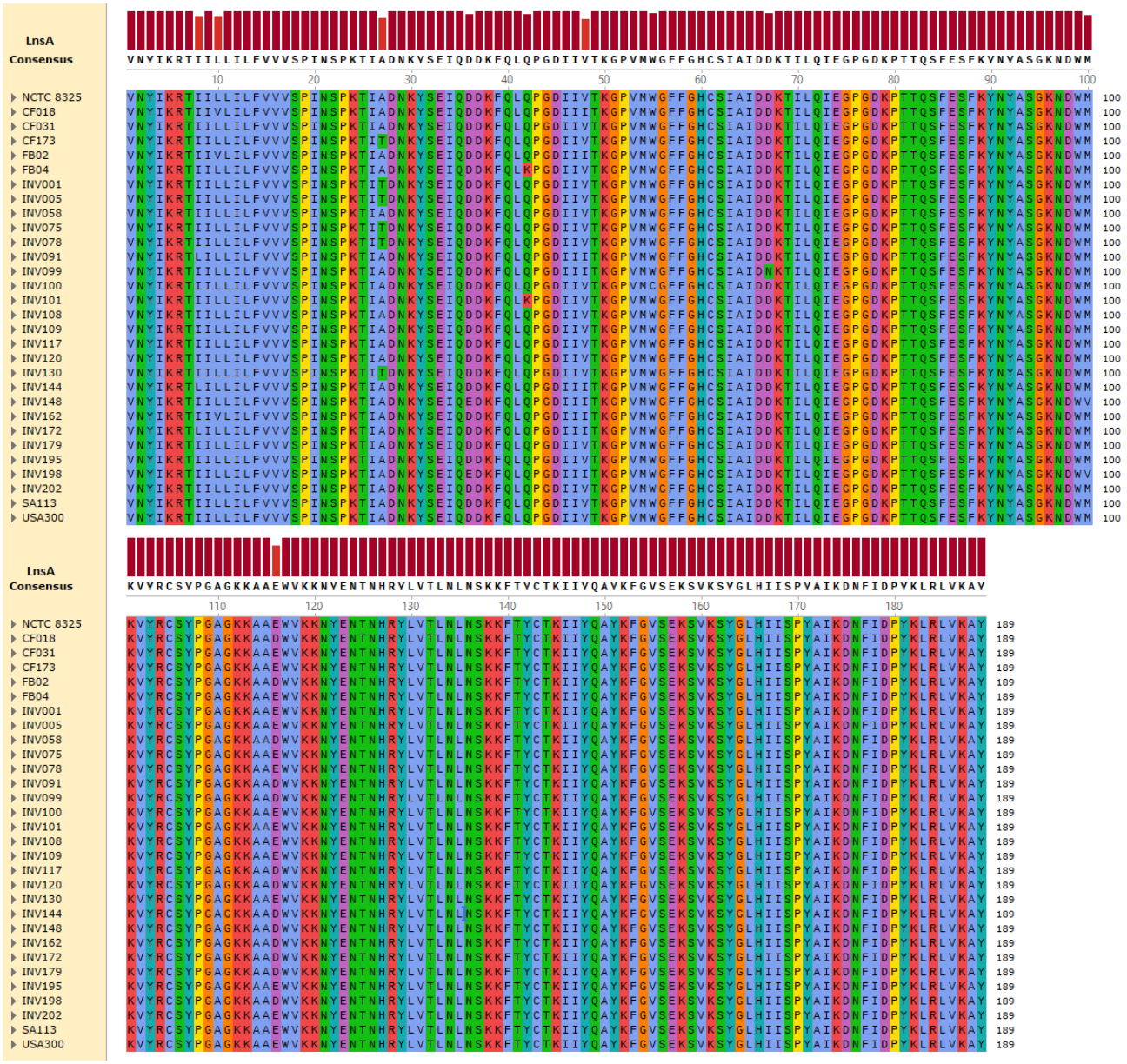

Figure 3.2: Protein alignment of *lnsA* sequence from *S. aureus* isolates. Translated *lnsA* sequences were aligned using the MUSCLE algorithm. The consensus protein sequence is shown above the alignment, with red boxes depicting the level of consensus at every position. Amino acids were colour-coded according to their functionality (red = positively charged, purple = negatively charged, green = polar, blue = hydrophobic, turquoise = aromatic, orange = glycine, and yellow = proline). The *lnsA* locus of CF014 was unable to be sequenced and is not included in the alignment.

Within the 30 clinical isolates, non-conserved amino acid substitutions occurred at only three positions: A27T (hydrophobic alanine to polar uncharged threonine at amino acid position 27)

present in ST225 and ST2112, Q42K (polar uncharged glutamine to positively charged lysine at amino acid position 42) present in CC22 and D67N (negatively charged aspartic acid to polar uncharged asparagine) present in ST2815. Compared with the conserved sequence of the gene, the upstream mRNA region between the predicted *InsA* promoter site and the *InsA* start codon showed greater sequence diversity (Figure 3.3).

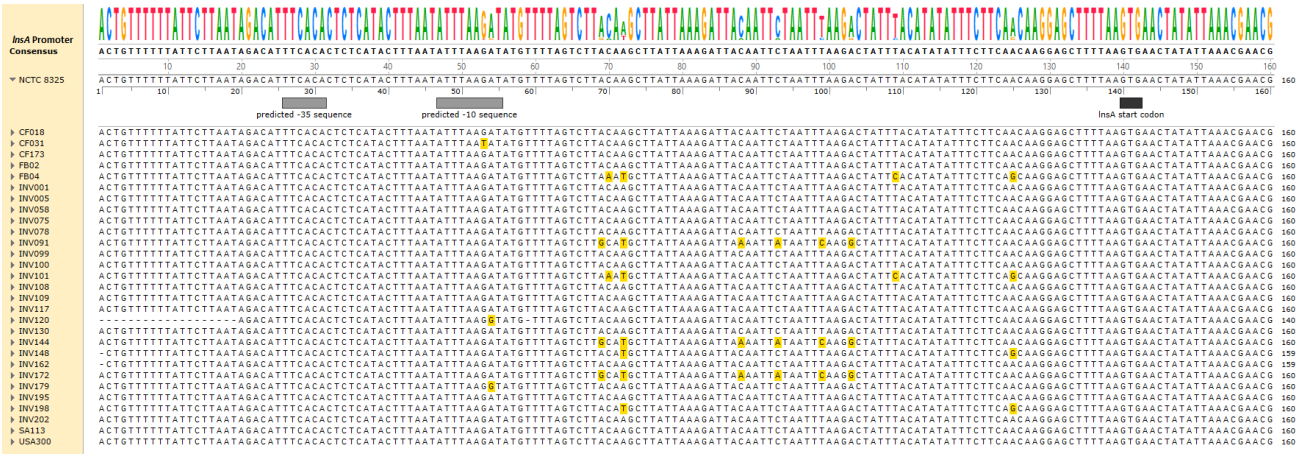

Figure 3.3: MUSCLE alignment of the upstream *InsA* sequences from *S. aureus* isolates. The -10 and -30 promoter sequences were predicted by software BPROM using the reference NCTC 8325 sequence. Nucleotides that differ from the consensus sequence are shown in gold. The *InsA* locus of CF014 was unable to be sequenced and is not included in the alignment.

In contrast, the *InsB* locus showed much greater diversity (Figure 3.4).

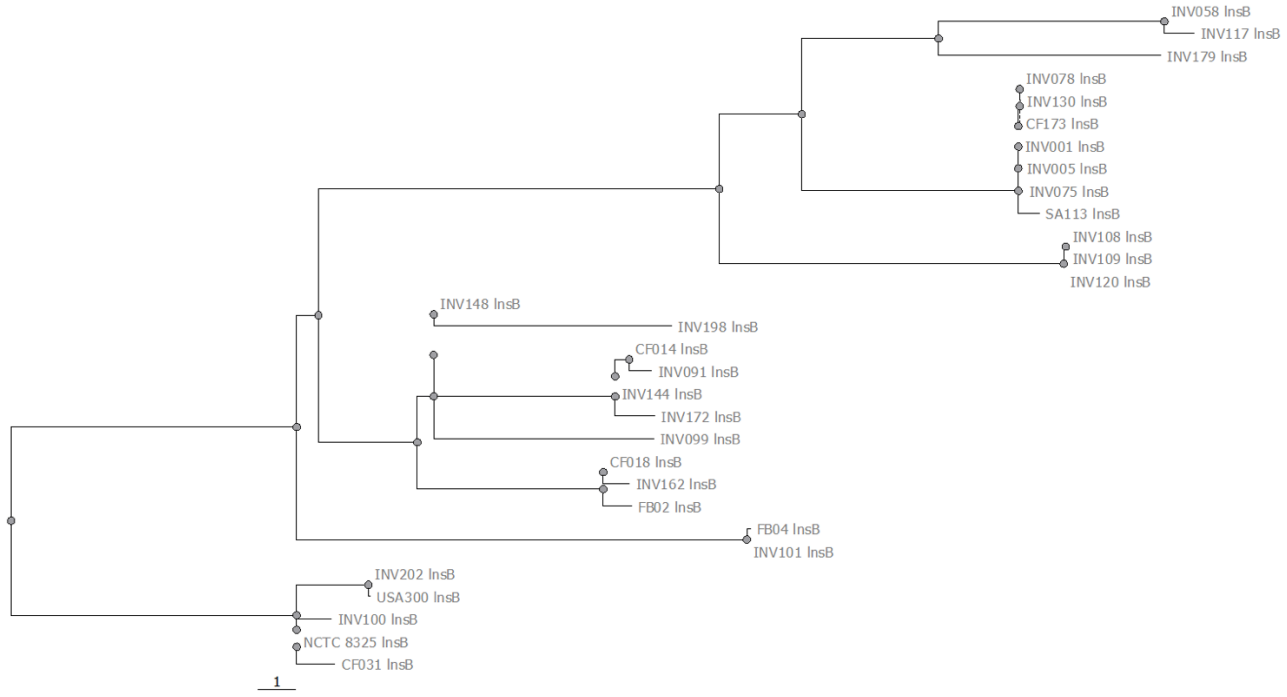

Figure 3.4: Phylogenetic tree of the *InsB* locus. The *InsB* locus of INV195 was unable to be sequenced and is not included in this phylogenetic tree.

Translating the *InsB* gene sequence into an amino acid sequence showed several non-conserved amino acid substitutions (Figure 3.5). LnsB is predicted to be a membrane associated protein (Smithers et al., 2021). The observed non-conserved substitutions occured not in hydrophobic regions of the protein and are therefore assumably not part of the membrane bound part.

Figure 3.5: Protein alignment of *lnsB* sequence from *S. aureus* isolates. Translated *lnsB* sequences were aligned using the MUSCLE algorithm. The consensus protein sequence is shown above the alignment with red boxes depicting the level of consensus at every position. Amino acids were colour-coded according to their functionality (red = positively charged, purple = negatively charged, green = polar, blue = hydrophobic, turquoise = aromatic, orange = glycine, and yellow = proline). The *lnsB* locus of INV195 was unable to be sequenced and is not included in the alignment.

3.2 Expression of *lnsA* and *lnsB* is significantly downregulated in low pH

To understand the role of *lnsA* and *lnsB* in lipoprotein modification under stress-inducing conditions, the expression of the two genes was measured in different growth conditions using RT-PCR. Expression of *lnsA* and *lnsB* was quantified in bacteria grown in low pH. (Figure 3.6). The experiment was done twice (named “first experiment” and “second experiment”) under the same conditions. Almost every experiment was performed twice and is denoted that way. Expression of *lnsA* and *lnsB* in *S. aureus* isolates grown in pH 7.3 was set to 1. Gene expression in pH 5.5 is shown as relative expression compared to pH 7.3. Both genes were overall significantly downregulated in low pH in both experiments. *lnsA* mRNA levels significantly decreased an average of 1.5-fold and 2.8-fold. *lnsB* mRNA levels significantly decreased an average of 1.3-fold and 2-fold. Gene expression of the population of 30 isolates in total went down. Some isolates showed no change in gene expression amongst other isolates showing a strong decrease.

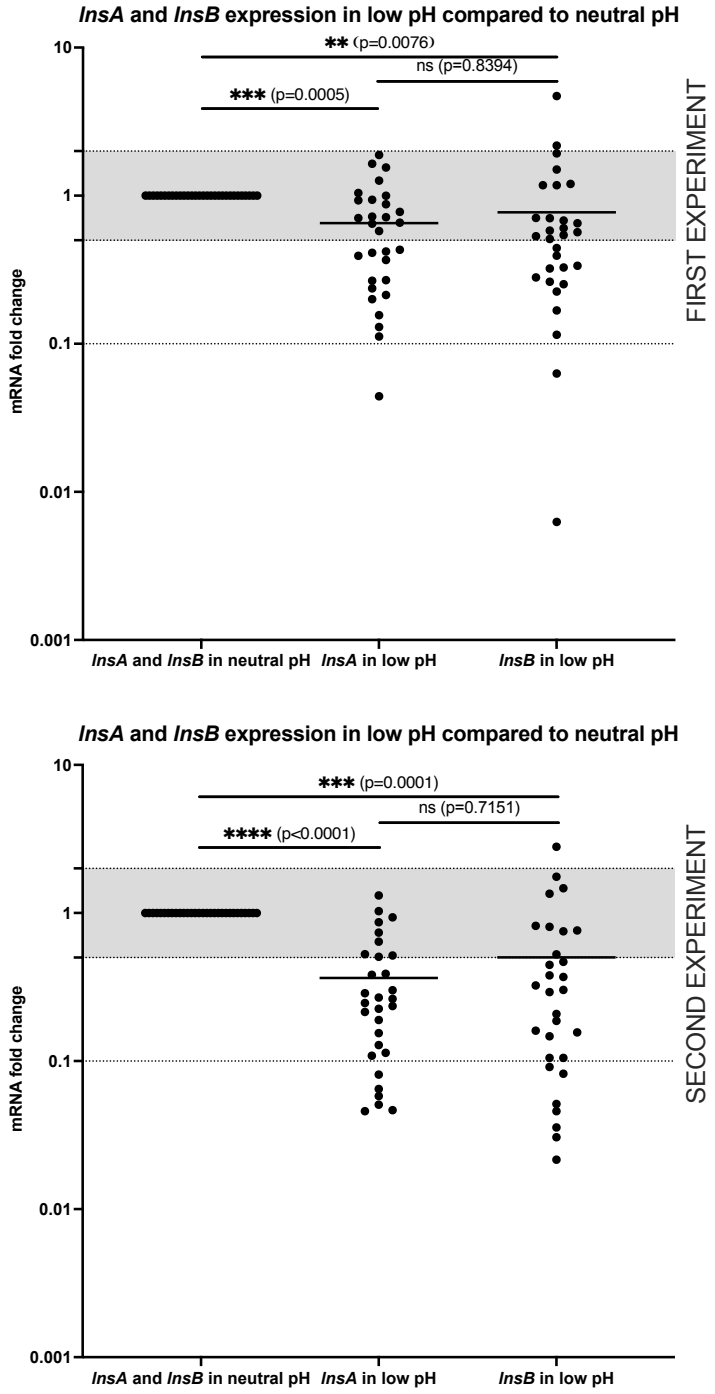

Figure 3.6: Relative gene expression of *InsA* and *InsB* in *S. aureus* grown in a low pH environment (pH 5.5) compared to a neutral pH environment (pH 7.3). Gene expression was quantified by RT-PCR. The two graphs derive from independent experiments. Each dot represents one *S. aureus* isolate, bars indicate the mean. Horizontal dotted lines are drawn at y=0.1, 0.5 and 2. The grey area between y=0.5 and y=2 illustrates a +/- 2-fold change.

3.3 Expression of *lnsA* and *lnsB* is significantly downregulated in high salt

In accordance with the previous experiment in low pH, *lnsA* and *lnsB* expression was quantified in *S. aureus* strains grown in high salt concentrations (1 M NaCl) compared to low salt concentrations (0.086 M NaCl) (Figure 3.7). Gene expression in low salt concentrations was set to 1. Gene expression in high salt concentrations is shown as relative expression. Both genes were significantly downregulated in high salt in both experiments. *lnsA* mRNA levels significantly decreased an average of 3-fold and 2.2-fold. *lnsB* mRNA levels significantly decreased an average of 2.2-fold and 2-fold. Just like for the observed change in gene expression in low pH, the observed down-regulation in high salt accounted for the entire population of 30 isolates, despite single isolates showing a weak increase or no change in gene expression. Overall, the observed downregulation in high salt concentrations was stronger than the downregulation in the low pH environment.

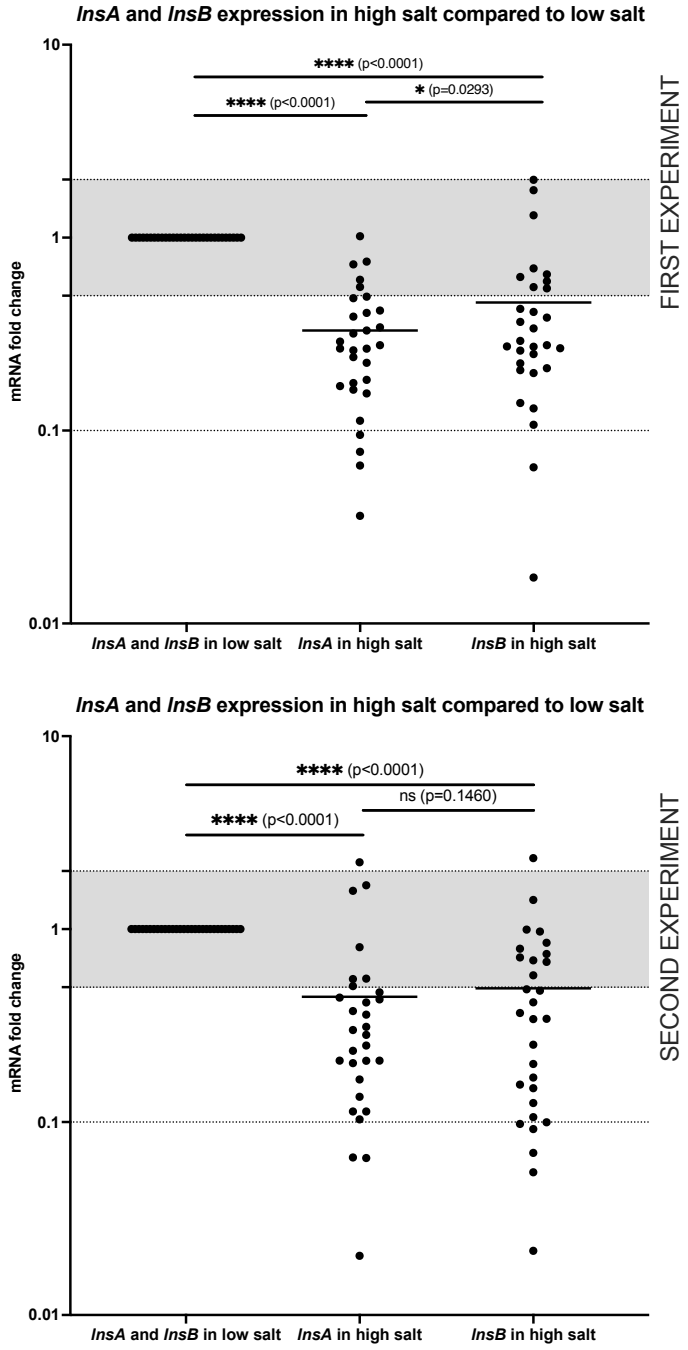

Figure 3.7: Relative gene expression of *InsA* and *InsB* in *S. aureus* grown in high salt concentrations (1 M NaCl) compared to low salt concentrations (0.086 M NaCl). Gene expression was quantified by RT-PCR. The two graphs derive from independent experiments. Each dot represents one *S. aureus* isolate, bars indicate the mean. Horizontal dotted lines are drawn at y=0.1, 0.5 and 2. The grey area between y=0.5 and y=2 illustrates a +/- 2-fold change.

3.4 Expression of *InsA* and *InsB* in low pH and high salt concentrations might be regulated by different factors

To investigate if the isolates, that showed the greatest change in gene expression under low pH conditions, were the same as those showing the greatest change in high salt concentrations, the correlation of gene expression between those different conditions was analyzed for *InsA* and *InsB*. (Annex, Figure 6.1). No strong correlation was observed. Calculating the spearman correlation coefficient for the relative *InsA* expression in low pH and relative *InsA* expression in high salt concentrations resulted in $r_s = 0.4536$ and $r_s = 0.2836$. Calculating the spearman correlation coefficient for the relative *InsB* expression in low pH and relative *InsB* expression in high salt concentrations resulted in $r_s = 0.3303$ and $r_s = 0.6044$.

3.5 Expression of *InsA* and *InsB* is not significantly influenced by cell wall active antibiotic ampicillin

InsA and *InsB* expression was furthermore quantified in *S. aureus* cells grown in the presence of ampicillin (100 µg/µL), since subinhibitory concentrations of β-lactam-antibiotics have been shown to play a role in the expression of lipoprotein-like genes and the immune recognition by human TLR2 (Shang et al., 2019). Figure 3.8 shows the relative expression of *InsA* and *InsB* in 23 isolates grown in the presence of cell wall active ampicillin compared to growth in media without the drug. Notably, five isolates were sensitive to ampicillin (SA113 is known to be sensitive, INV117, INV099, INV148 and INV058 were tested by antibiogram) and could therefore not be grown in the presence of the drug. Four isolates showed growth, despite impaired growth rates (determined by OD_{600}) in the presence of the antibiotic and were harvested later to ensure harvesting in stationary phase (INV101 and INV162 after 24 hours, INV120 and INV109 after 40 hours). Furthermore, INV005 and INV130 dropped out due to technical problems. *InsA* and *InsB* mRNA levels were not significantly influenced by the presence of ampicillin. Expression levels of *InsA* and *InsB* in the presence of ampicillin occurred in most of the isolates within a two-fold range (within the grey area in Figure 3.8). Since ampicillin caused no considerable effect on gene expression within this population, this experiment was not repeated.

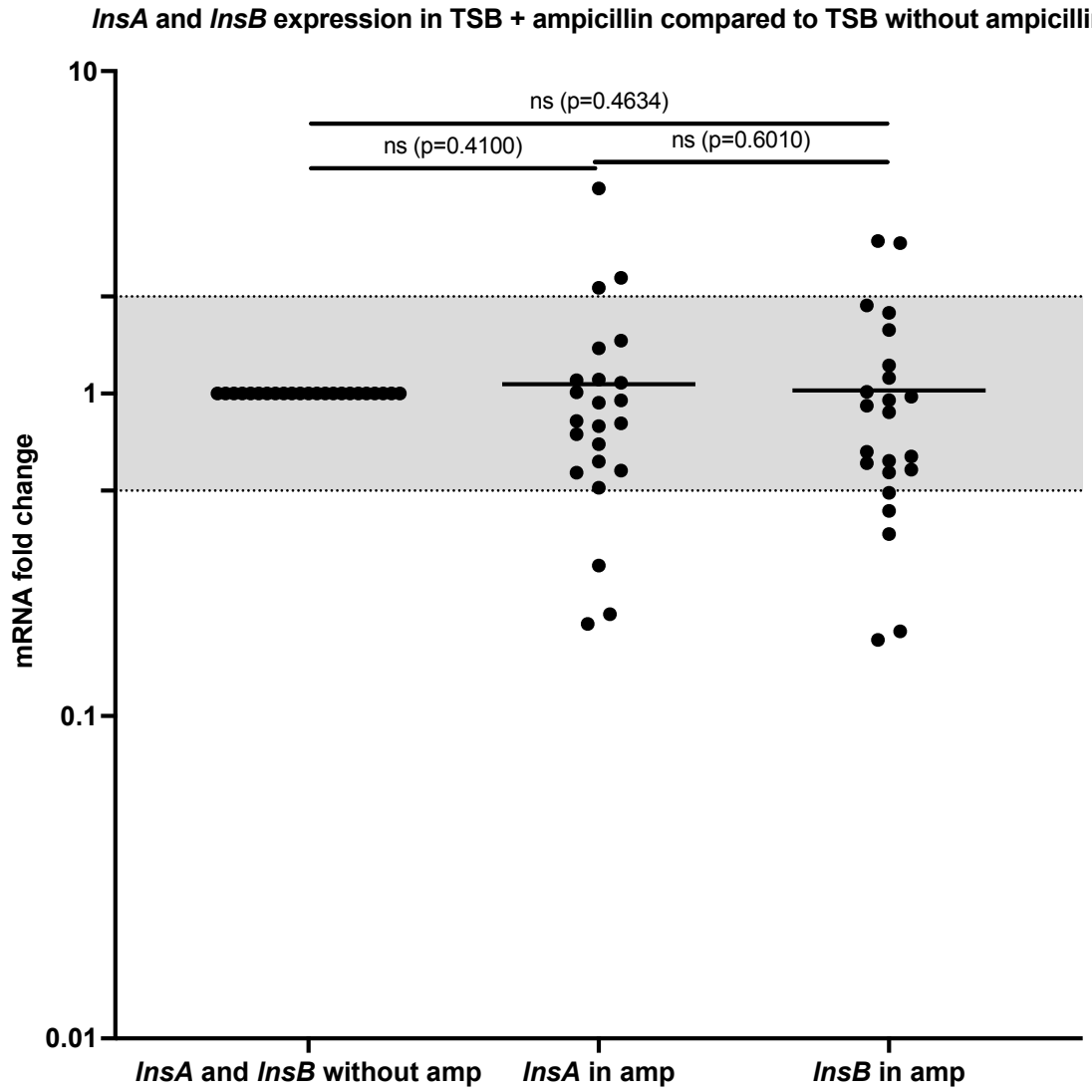

Figure 3.8: Relative gene expression of *InsA* and *InsB* in *S. aureus* isolates grown in the presence of ampicillin (amp) to cells grown without the presence of the antibiotic. Gene expression was quantified by RT-PCR. Each dot represents one *S. aureus* isolate, bars indicate the mean. The grey area illustrates a +/- two-fold change.

3.6 The expression of *InsA* and *InsB* appears to be correlated

The change in *InsA* and *InsB* gene expression under different conditions (Figures 3.6 - 3.8) was similar and showed only a small difference in one of five experiments. To probe this observation, the correlation between the fold-change in *InsA* and *InsB* expression for each condition was graphed in Figure 3.9.

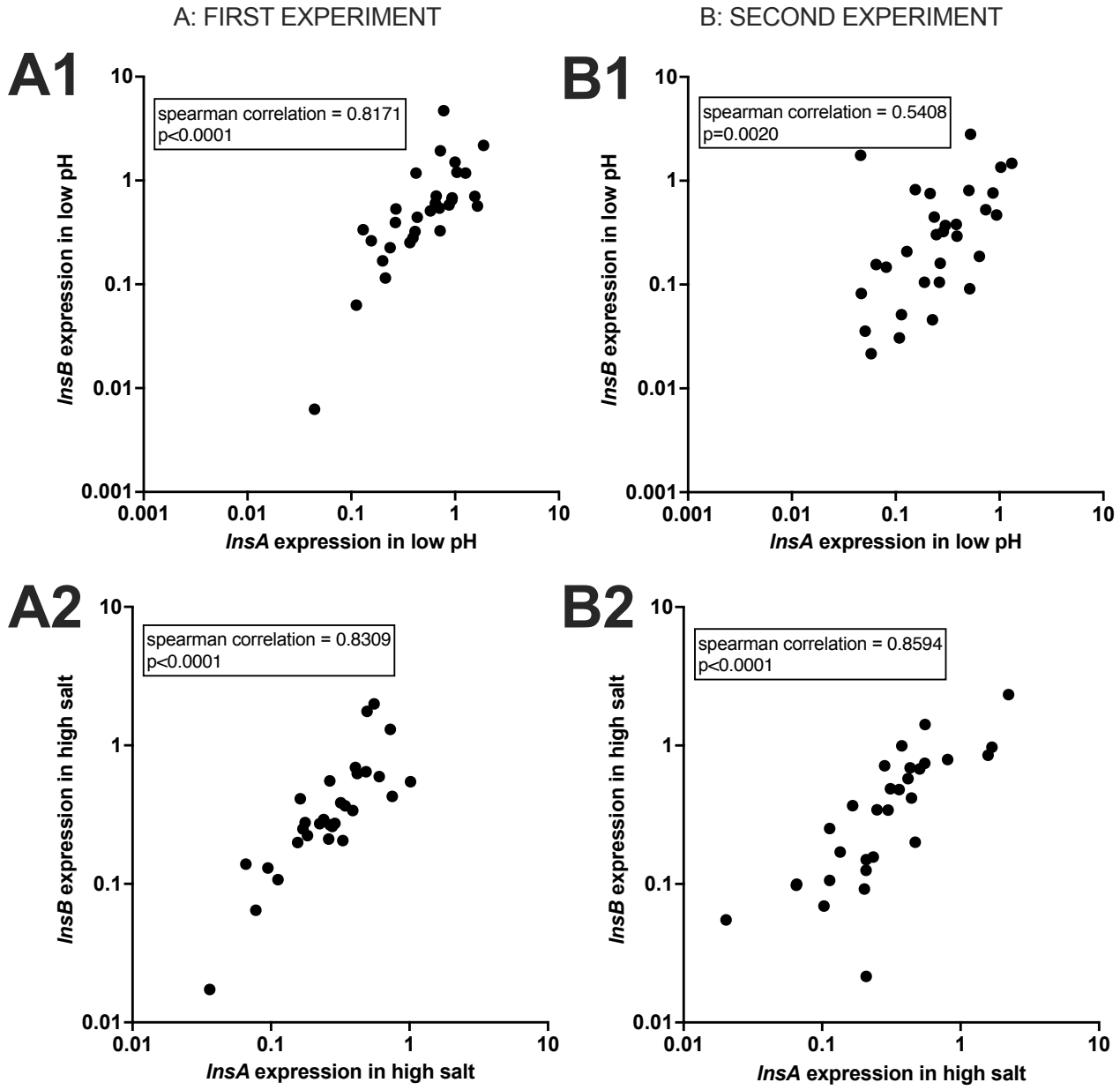

Figure 3.9: Correlation graphs of *InsA* and *InsB* under different conditions. Graphs A and B derive from independent experiments. Graphs A1 and B1 show the correlated expression of *InsA* and *InsB* in *S. aureus* isolates grown in low pH (pH 5.5) as relative expression to the expression in isolates grown in neutral pH (pH 7.3). Graphs A2 and B2 show the correlated expression of *InsA* and *InsB* in *S. aureus* isolates grown in high salt concentrations (1 M NaCl) as relative expression to the expression in bacteria grown in low salt concentrations (0.086 M NaCl).

The graphs show a linear correlation in the distribution of the population. Calculating the spearman correlation coefficient for the expression of *InsA* and *InsB* in low pH resulted in r_s= 0.8171 in the first experiment and r_s= 0.5408 in the second experiment. Calculating the spearman correlation coefficient for the expression of both genes in high salt concentrations resulted in r_s= 0.8309 in the first experiment and r_s= 0.8594 in the second experiment. Spearman correlation coefficient was therefore above 0.8 in three out of four experiments and above 0.5 in one experiment strongly indicating an overall correlation.

3.7 Expression of *S. aureus* glycerol ester hydrolase gene (*geh*) in low pH, high salt concentrations and in the presence of ampicillin

Because of its role in modifying *S. aureus* lipoproteins causing changes in TLR recognition, the expression of *S. aureus* lipase glycerol ester hydrolase gene (*geh*) was quantified in low pH, high salt concentrations and in the presence of ampicillin and compared to either neutral pH, low salt concentrations or TSB without ampicillin (Figure 3.10). In the first experiment, a significant difference for the population could not be observed under any condition. In the second experiment, *geh* expression significantly increased in low pH (mean 2.9-fold change) and in high salt (mean 3.9-fold change). Ampicillin as an experimental condition was not repeated in the second experiment due to the previously mentioned reasons.

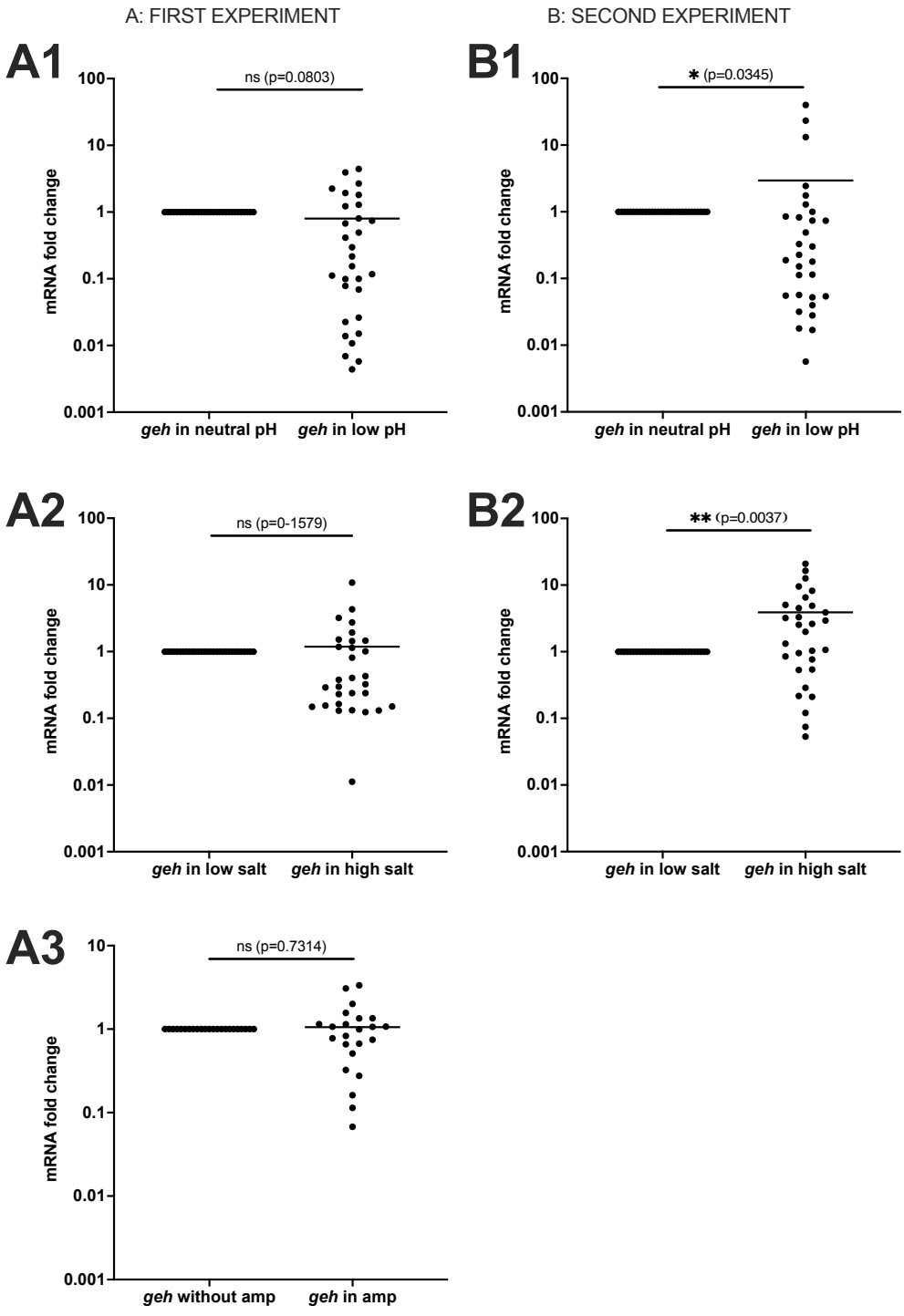

Figure 3.10: Expression of *geh* under different growth conditions (A1+B1 low pH, A2+B2 high salt, A3 ampicillin (amp)). Relative gene expression was quantified by RT-PCR. Graphs A and B derive from independent experiments. Each dot represents one *S. aureus* isolate, bars indicate the mean.

3.8 TLR2 induced IL-8 secretion is dependent on heterodimerization with TLR1 or TLR6

HEK293 cells transiently transfected with human TLR2 and additionally either TLR6, TLR1 602S or TLR1 602I, were stimulated with different synthetic ligands (Figure 3.11). The different TLR1 variants were used since TLR1 602S is internalized and not sufficient to detect tri-acylated lipoproteins. It was used to detect a non-specific signal or a signal generated by TLR2 in a TLR1/6 independent manner. TLR1 602I is present on the cell surface and together with TLR2 sufficient in the detection of tri-acylated lipoproteins. TLR2 heterodimer activation was measured by IL-8-ELISA. The postulated distinction between TLR1 and TLR6 concerning the acylation state of their ligand was clearly shown. Pam_2CSK_4, a synthetic ligand imitating di-acylated lipoproteins, induced the strongest IL-8 secretion in HEK293 cells expressing TLR2 and TLR6, while Pam_3CSK_4, a synthetic ligand imitating tri-acylated lipoproteins, induced the strongest IL-8 secretion in HEK293 cells expressing TLR2 and TLR1 602I. Pam_2CSK_4 induced the strongest IL-8 secretion in cells expressing TLR2 and TLR6, followed by an approximately equal signal in cells expressing TLR2 plus either TLR1 602S or TLR1 602I. Pam_2CSK_4 therefore seems to not necessarily need TLR6 to induce a signal through TLR2 and the activation of TLR2 can happen in a TLR1-independent or negligible way, since the signal was similar in cells presenting TLR1 on their surface (602I) and cells insufficient in trafficking TLR1 to their surface (602S). Similarly, *in vitro* data showed that lipoprotein SitC could induce TLR2 activity in a TLR1 or TLR6 independent manner. (Kurokawa et al., 2009) Nonetheless, a nonspecific receptor activation cannot be ruled out. Pam_3CSK_4 induced the strongest IL-8 secretion in HEK293 cells expressing TLR2 and TLR1 602I, followed by cells expressing TLR2 and TLR1 602S. HEK293 cells expressing TLR2 and TLR6 showed the lowest IL-8 secretion when stimulated with Pam_3CSK_4. Pam_1CSK_4, a synthetic ligand that consists of a single fatty acid attached to a small peptide's N-terminus, did not sufficiently activate any TLR. Therefore, a single acyl chain attached to a peptide does not function as a TLR2/1/6 ligand and the binding of a peptide to TLR2/1/6 is dependent on at least two acyl chains (di-acylated). Also, the detected signal derived from the acylated peptides indeed and HEK293 cells were not responding to some other unknown factor.

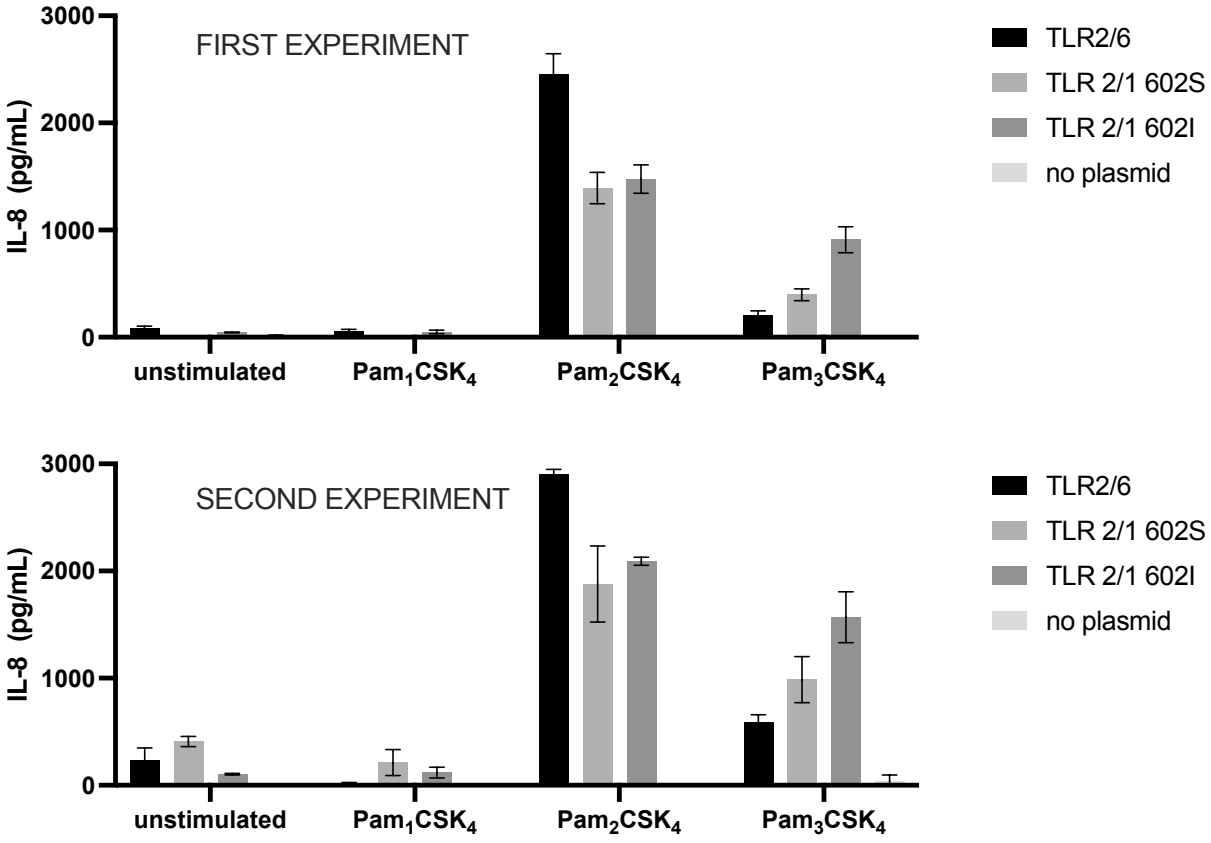

Figure 3.11: Stimulation of HEK293 cells co-expressing different TLRs. The two graphs derive from independent experiments. Error bars derive from biological triplicates from three stimulations. Two types of negative controls were included. Firstly, HEK293 cells, that had not been transfected, were stimulated. Secondly, transfected HEK293 cells were incubated without a stimulus. In the first experiment, IL-8 secretion in the negative controls was below the detection threshold. In the second experiment, IL-8 secretion of the negative controls showed a weak signal.

3.9 Low pH strongly decreases IL-8 secretion in HEK293 cells expressing TLR2 and TLR1 on their surface

Next, this system was used to analyze TLR2 activity upon exposure to bacterial cells grown in low pH. To this end, HEK293 cells transiently transfected with human TLR2 and additionally either TLR6, TLR1 602S or TLR1 602I, were stimulated with protein lysates of *S. aureus* isolates grown either in neutral pH (pH 7.3) or low pH (pH 5.5) (Figure 3.12). Stimulations

were performed with *S. aureus* protein lysates since bacterial lipoproteins are attached to the membrane and a lysate might enable an easier detection by TLRs.

HEK293 cells expressing TLR2 and TLR1 on their surface (TLR1 602I) showed a significant decrease in IL-8 secretion when stimulated with bacterial lysates from bacteria grown in low pH compared to neutral pH. IL-8 secretion was at mean 1400 pg/mL when stimulated with lysates of bacteria grown in neutral pH and dropped to mean 1023 pg/mL when stimulated with lysates of bacteria grown in low pH in the first experiment. The second experiment showed an IL-8-drop from mean 1750 pg/mL to mean 841 pg/mL. This observed decrease was specific to TLR1, since the internalization of TLR1 (TLR1 602S) omitted the effect: IL-8-secretion in HEK293 cells expressing TLR2 and TLR1 602S decreased only modest but significant from mean 1071 pg/mL when stimulated with bacteria grown in basic pH to mean 941 pg/mL when stimulated with bacteria grown in low pH. The replication of the experiment showed a decrease from mean 509 pg/mL to mean 383 pg/mL. The extent of this shift is not comparable with the shift in HEK203 cells expressing TLR1 on their surface.

IL-8-secretion in HEK293 cells expressing TLR2 and TLR6 significantly increased from mean 1107 pg/mL when stimulated with *S. aureus* isolates grown in neutral pH to mean 1261 pg/mL when stimulated with isolates grown in low pH. The replication of the experiment showed a non-significant increase (mean 622 to 743 pg/mL).

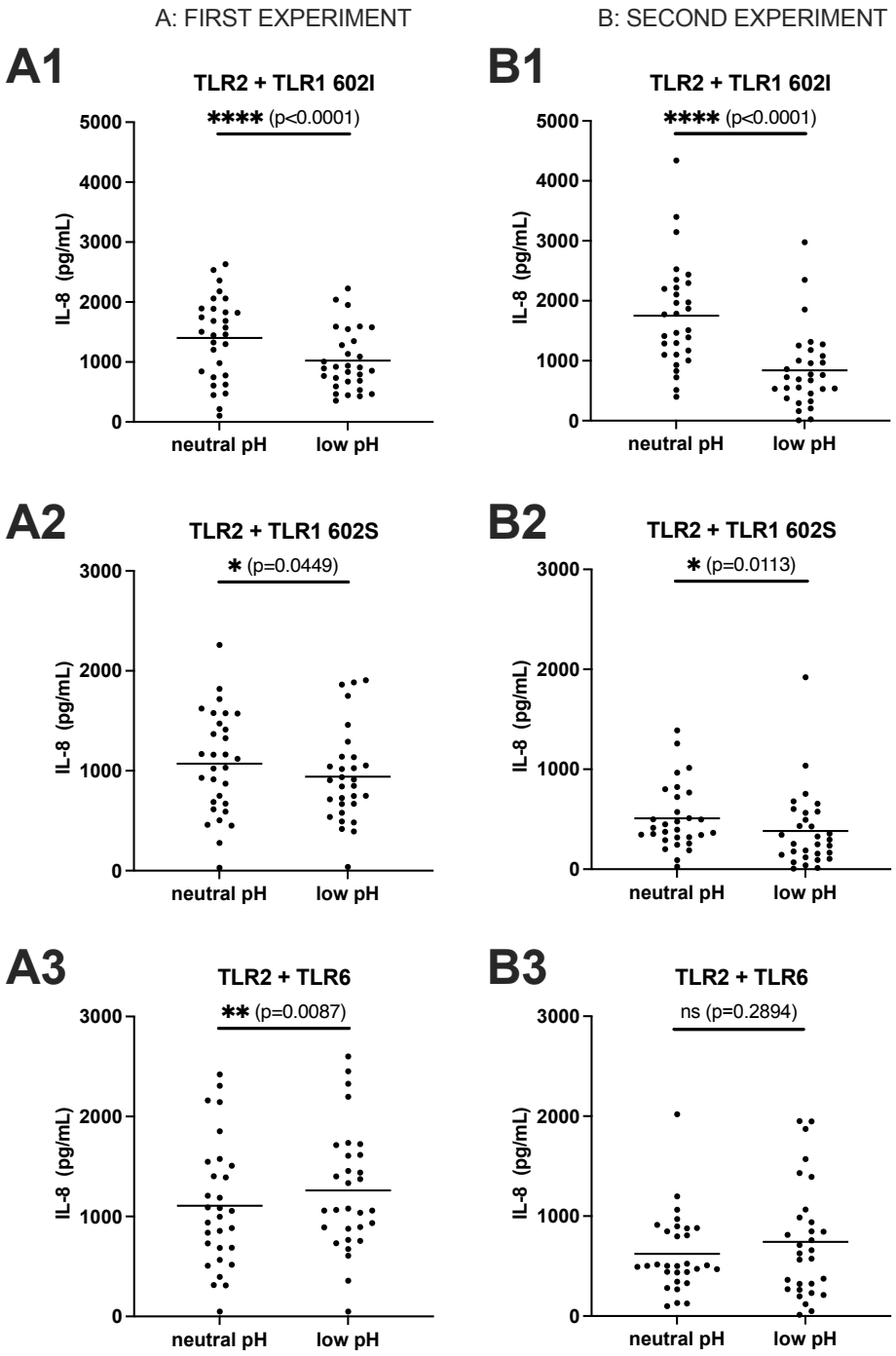

Figure 3.12: Stimulation of HEK293 cells expressing TLR2 and additionally either TLR1 602I (A1, B1), TLR1 602S (A2, B2) or TLR6 (A3, B3) with protein lysates of the 30 *S. aureus* isolates grown either in neutral pH (pH 7.3) or low pH (pH 5.5). Graphs A and B derive from independent experiments. Each dot represents the mean of a stimulation triplicate of one isolate. Bars show the mean of the population of 30 isolates.

3.10 High salt exposure significantly increases IL-8 secretion in HEK293 cells expressing TLR2 and TLR6

Similar to the experimental set up described in the previous chapter, HEK293 cells transiently transfected with human TLR2 and additionally either TLR6, TLR1 602S or TLR1 602I, were this time stimulated with protein lysates of *S. aureus* isolates grown either in low (0.086 M NaCl) or high (1 M NaCl) salt concentrations (Figure 3.13). IL-8 secretion in HEK293 cells expressing TLR2 and TLR6 significantly increased when stimulated with *S. aureus* isolates grown in high salt concentrations compared to low salt concentrations. In the first experiment, IL-8 secretion increased from mean 1107 pg/mL when stimulated with lysates of bacteria grown in low salt concentrations to mean 1316 pg/mL when stimulated with lysates of bacteria grown in high salt concentrations. The second experiment showed an increase from mean 622 pg/mL to mean 1161 pg/mL. The increase was significant in both experiments.

HEK293 cells expressing TLR2 and TLR1 602S showed no significant change in IL-8 secretion between the two stimuli in the first experiment (means 1071 and 1050 pg/mL). In the second experiment, IL-8 secretion increased modest but significant from mean 509 pg/mL when stimulated with *S. aureus* isolates grown in low salt concentrations to mean 714 pg/mL when stimulated with isolates grown in high salt concentrations.

In HEK293 cells expressing TLR2 and TLR1 602I, IL-8 secretion significantly decreased from mean 1400 pg/mL when stimulated with bacteria grown in low salt concentrations to mean 1193 pg/mL when stimulated with bacteria grown in high salt concentrations in the first experiment The second experiment showed no significant change (means 1750 and 1783 pg/mL).

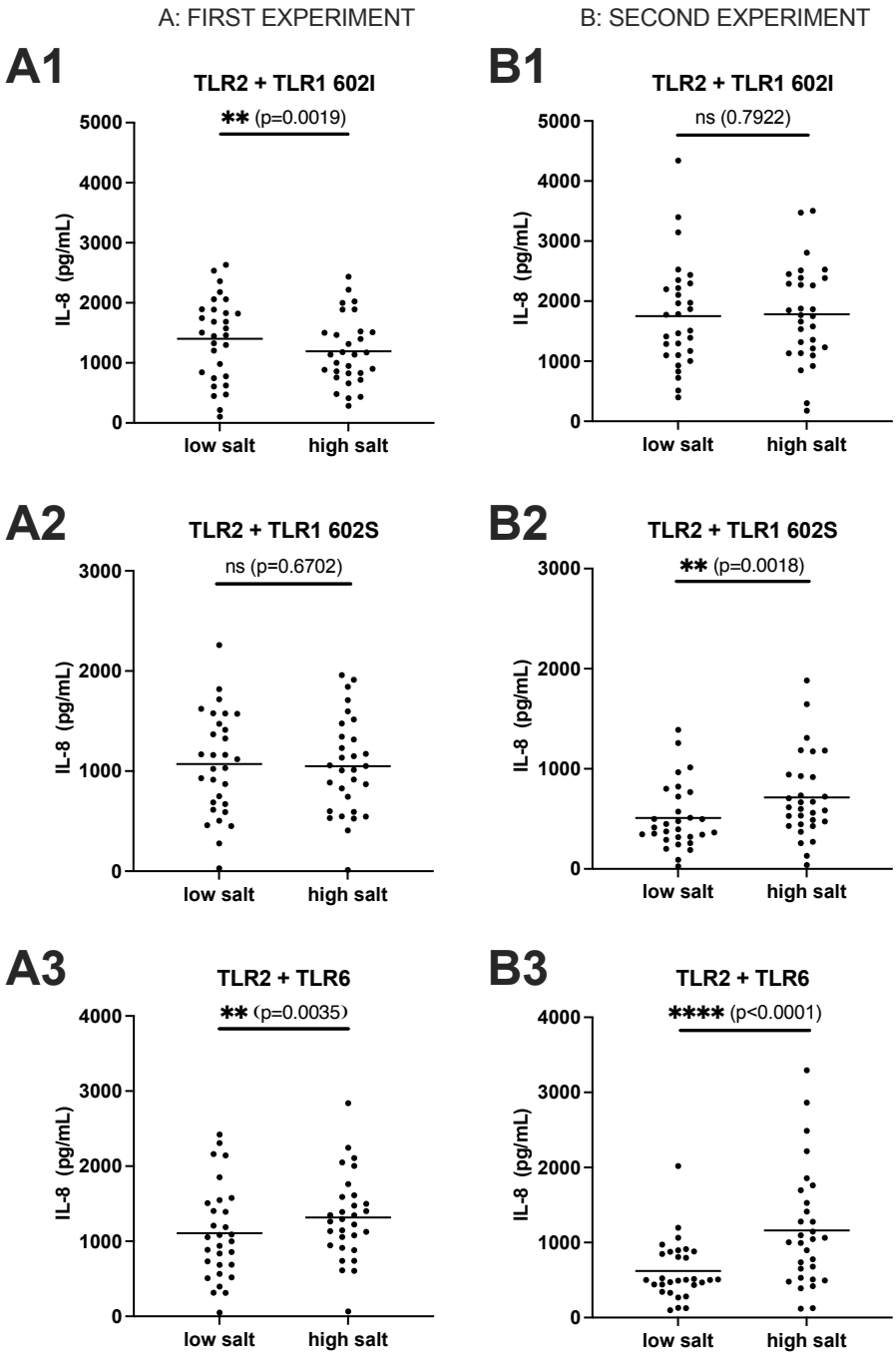

Figure 3.13: Stimulation of HEK293 cells expressing TLR2 and additionally either TLR1 602I (A1, B1), TLR1 602S (A2, B2) or TLR6 (A3, B3) with protein lysates of the 30 *S. aureus* isolates grown either in low salt concentrations (0.086 M NaCl) or high salt concentrations (1 M NaCl). Graphs A and B derive from independent experiments. Each dot represents the mean of a stimulation triplicate of one isolate. Bars show the mean of the population of 30 isolates.

3.11 β-lactam ampicillin does not affect TLR2/1/6 signal

In agreement to the experimental set up described in chapters 3.9 and 3.10, HEK293 cells transiently transfected with human TLR2 and additionally either TLR6, TLR1 602S or TLR1 602I, were this time stimulated with protein lysates of 24 *S. aureus* isolates grown either in the presence of ampicillin or without the drug (Figure 3.14). This experiment includes the same set of isolates as the RT-PCR experiment with ampicillin. IL-8 secretion did not change significantly in any of the transfected HEK293 cells. Because of the absent effect and limited time, this experiment was not repeated.

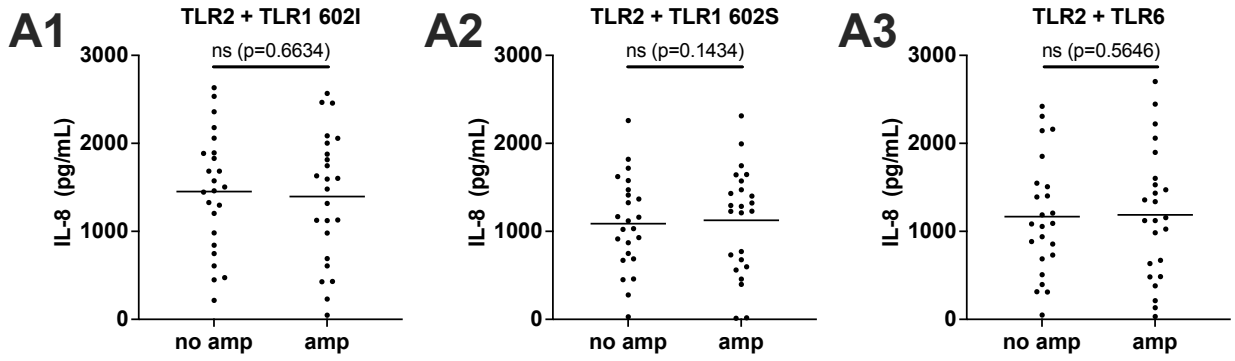

Figure 3.14: Stimulation of HEK293 cells expressing TLR2 and additionally either TLR1 602I (A1), TLR1 602S (A2) or TLR6 (A3) with protein lysates of 24 *S. aureus* isolates grown either in the presence of ampicillin (amp) (100 µg/mL) or without the presence of the drug. Each dot represents the mean of a stimulation triplicate of one isolate. Bars show the mean of the population of 24 isolates.

3.12 Changes in TLR specificity occur for the population of 30 isolates in a coherent manner

To further understand the changes in TLR specificity that occurred through different bacterial growth conditions, absolute IL-8 values were converted to relative values (Figure 3.15). *S. aureus* isolates grown in low pH showed a strong decrease in their TLR2/1 activation capacity in almost all isolates. The population clearly shifted down on the y-axis. TLR2/6 activation was not affected in a similar obvious trend. Most isolates showed an increase, while some showed a decrease in receptor activation. *S. aureus* isolates grown in high salt concentrations showed a different effect on TLR specificity. The population clearly showed a stronger TLR2/6 signal. The population shifted to the right on the x-axis. The effect on TLR2/1

activation was more ambiguous. While many isolates showed an impaired TLR2/1 activation capacity, other isolates showed stronger TLR2/1 activation. Whether or not bacteria were grown in the presence of ampicillin seemed to not affect their TLR specificity. The population was very conserved around x=y=1. The outlier on the bottom left quadrant was isolate CF014. Technical issues cannot be ruled out for this isolate since the experiment in ampicillin was not repeated. Under all conditions, the collection of 30 isolates seemed conserved and occurred as one population, aside from single outliers. There was no trend for distinction of sub-populations.

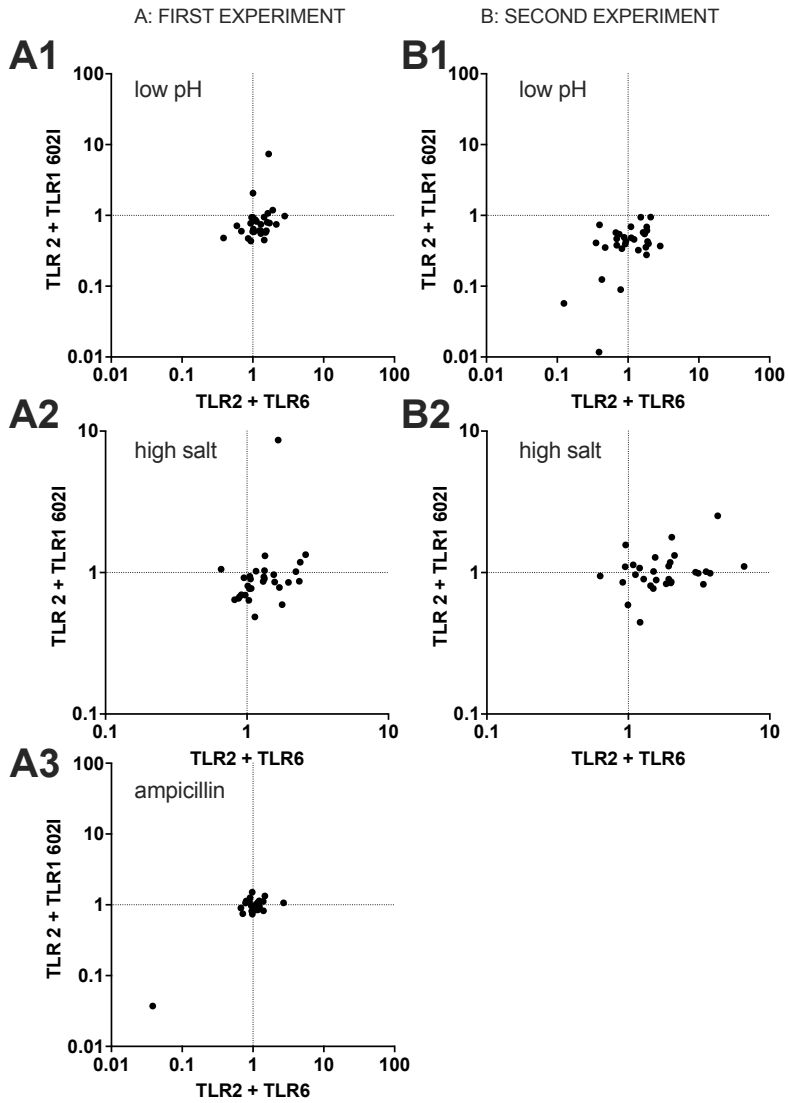

Figure 3.15: Relative Toll-like receptor activation by *S. aureus* isolates grown under different conditions. Graphs A and B derive from different experiments. Each dot represents one isolate. X-values derive from secreted IL-8 of HEK293 cells transfected with TLR2 and TLR6 stimulated with bacteria grown under a certain condition divided by secreted IL-8 of HEK293 cells transfected with TLR2 and TLR 6 stimulated with bacteria grown in regular TSB without supplements. Y-values derive from secreted IL-8 of HEK293 cells transfected with TLR2 and TLR1 602I stimulated with bacteria grown under a certain condition divided by secreted IL-8 of HEK293 cells transfected with TLR2 and TLR1 602I stimulated with bacteria grown in regular TSB without supplements. A1+B1) Relative TLR activation in HEK293 cells stimulated with bacteria grown in low pH compared to neutral pH. A2+B2) Relative TLR activation in HEK293 cells stimulated with bacteria grow in high salt concentrations compared to low salt concentrations. A3) Relative TLR activation in HEK293 cells stimulated with bacteria grown in the presence of ampicillin compared to bacteria grown without the drug.

4 Discussion

This work is based on 30 clinical *S. aureus* isolates from different sources (Table 2.1). The isolates differed in the expression of virulence and resistance-encoding factors: 12 isolates were classified as *mecA* encoding MRSA, four isolates contained Panton-Valentine leucocidin (Table 2.4). The *S. aureus* isolates originated from six different clonal complexes and 16 different strain types (Table 2.7). To understand whether this diversity was also reflected by the sequences of *lnsA* (SAOUHSC_00822) and *lnsB* (SAOUHSC_02761), the loci of both genes were sequenced. While the *lnsA* locus was highly conserved, the *lnsB* locus showed a number of mutations leading to several non-conserved amino acid substitutions. Mutations in both loci were associated with clonal complexes in a stronger sense for the *lnsB* locus than for the *lnsA* locus.

To understand if differences within the gene sequences lead to differences in the expression of the genes, RT-PCR experiments were performed. The results showed no transferable effect of *lnsA* and *lnsB* locus mutations on the genes' expressions.

Both LnsA and LnsB enzymes are required for maturation of *S. aureus* lipoproteins to the tri-acylated form (Gardiner et al., 2020). Moreover, Gardiner et al. demonstrated that neither gene regulates expression of the other (Gardiner et al., 2020). Notably, both genes are located within different genomic loci, on different strands (*lnsA* on the negative strand, *lnsB* on the positive strand) and are more than 1.7 million base pairs apart. However, within the analyses performed here, the expression of both genes appeared to correlate under the conditions tested (Figure 3.9), indicating that their expression might be similarly regulated. However, not much is known about the regulation of both genes. Knock-out experiments of gene regulators are needed to understand the underlying effects, but this was not the scope of this work. Nevertheless, in the context of the enzymes' codependent function, a common regulation mechanism is probably.

To investigate the function of *lnsA* and *lnsB* under cell stress-inducing conditions, gene expression was quantified in bacteria grown in low pH and high salt concentrations. Bacterial growth under both conditions led to decreased expression of *lnsA* and *lnsB* (Figures 3.6 and

3.7). The overall downshift observed among the isolates was significant in low pH and high salt concentrations, despite single outliers that were not all reproducible upon repetition of the experiment. The variability, that occurred within the *lnsB* sequence, did not translate to gene expression. Interestingly, the decrease in expression of *lnsA* and *lnsB* in cell stress-inducing conditions low pH and high salt concentrations appeared with a different magnitude at the level of an isolate. (Annex, Figure 6.1). The regulation can only be speculated at this point, but the data suggests that expression of the genes might be regulated by different factors in low pH and high salt concentrations.

Having examined the genetics of lipoprotein modifying enzymes, the next step was to look at potential downstream consequences concerning the lipoprotein phenotype and potential changes in TLR signaling.

LnsA and LnsB cooperate to produce the tri-acylation of lipoproteins, thus turning these into ligands for the TLR2 plus TLR1 heterodimer. If *lnsA* and *lnsB* were the only players involved, one would thus expect a decreased TLR2/1 activation in the absence or with reduced expression. Indeed, Gardiner et al. discovered that both genes were responsible for the generation of tri-acylated lipoproteins by generating ∆*lnsA* ∆*lnsB* double mutants and subsequently observing a reduced TLR2/1 signal and an increased TLR2/6 signal (Gardiner et al., 2020).

In this work, the expected correlation of enzyme expression and TLR2 heterodimer activation could be observed with some variation in magnitude under different conditions. Although *lnsA* and *lnsB* expression was strongly decreased in low pH and high salt concentrations and resulted in changes in TLR2 heterodimer preference, the intensity of TLR2/1 signal reduction and the inverse increase in TLR2/6 signal, both measured via IL-8 secretion, differed between the two conditions.

Of note, HEK293 cells expressing TLR2 and TLR1 on their surface (TLR1 602I) secreted significantly less IL-8 when stimulated with bacteria grown in low pH (low *lnsA* and *lnsB* expression) compared to the stimulation with bacteria grown in neutral pH (high *lnsA* and *lnsB* expression). This decrease was specific to TLR1, since the internalization of TLR1

(TLR1 602S) omitted the effect. Meanwhile, the TLR2/6 signal increased, as expected, but not proportionally to the TLR2/1 decrease. Consequently, in our cell system the loss of tri-acylated TLR2/1 signal was not replaced by an equivalently strong di-acylated TLR2/6 signal (Figure 3.12). However, the interpretation of these data should be performed with great caution because multiple ill-defined variables including spatio-physical differences in the positioning of the di- and tri-acylated lipoproteins in the cell membrane or differences in the expression or localization of the TLRs on the cell surface might influence these results and cannot be stringently controlled.

The effect of *lnsA* and *lnsB* downregulation was even stronger in bacteria grown in high salt concentrations, which fits well with the superb adaptation of *S. aureus* to high salt concentrations (Feng et al., 2022). Interestingly, using high salt-exposed isolates as a stimulus for TLR2-transfected HEK293 cells did not result in a strong decrease of TLR2/1-mediated IL-8 secretion, but was rather reflected by a TLR2/6 increase (Figure 3.13). Although these results, again, confirm that changes in *lnsA* and *lnsB* expression correlate with altered TLR2 heterodimer responsiveness, they indicate that unknown modulating factors orchestrate the lipoprotein-TLR interaction depending on the experimental conditions.

In Gardiner et al.'s publication, mutating *lnsA* and *lnsB* led to a strongly impaired TLR2/1 activity with an increased TLR2/6 activity. In this work, a significant downregulation of the genes led to a decreased TLR2/1 activity and an increased TLR2/6 signal with different intensities under different conditions and in different experiments. The observed changes in TLR specificity were not as clear, as observed with the double knockouts. However, despite the correlation, regulation seems to be more complex than initially expected. Thus, albeit tempting, it is not possible to predict whether the observations made in this study apply to the *in vivo* situation.

Amongst many, one factor worth talking about when looking at *S. aureus* lipoproteins as immunostimulatory TLR ligands is the lipase glycerol ester hydrolase (Geh). Geh is able to inactivate lipoproteins as TLR2 ligands (Chen & Alonzo, 2019). It has been demonstrated to perform ester hydrolysis on secreted *S. aureus* lipoproteins. In their experiments, the

inactivation occurred on Pam_2CSK_4 (TLR2/6 ligand) as well as Pam_3CSK_4 (TLR2/1 ligand) and was therefore not specific on TLR2's dimerization partner (TLR6 or TLR1). That being said, a concomitant increase in *geh* expression might be an explanation for reduced TLR2/1/6 stimulation, independent of the TLR2 dimerization partner. In this work, *geh* expression weakly varied between the first and the second experiment. In the first experiment, *geh* expression was unchanged in all conditions. In the second experiment, *geh* expression weakly increased in low pH and high salt (Figure 3.10). Thus, these findings are not expedient and cannot explain the absence of the decrease in TLR2/1 activation induced by bacteria grown high salt concentrations, nor of the expected strong TLR2/6 increase induced by bacteria grown in low pH conditions. It is well possible that uncontrolled varying expression of TLR2, TLR1 and TLR6 might influence the results but this could not be addressed within this thesis. Furthermore, membrane bound lipoproteins, which were not affected by Geh in Chen et al.'s publication, were used as stimuli in this work. Geh can therefore be ruled out to cause the main differences in TLR-mediated recognition of lipoproteins under the conditions tested in this work. Other factors involved can only be speculated. Another protein described to modulate Toll-like receptor responses to bacterial lipoproteins is the lipoic acid synthetase (LipA). Besides its function on the E2 subunit of the pyruvate dehydrogenase, it has been shown to attenuate *S. aureus* TLR2/1 signaling (Grayczyk et al., 2017).

Kurokawa et al. observed mainly di-acylated lipoproteins in low pH, but not high salt concentrations (Kurokawa, Kim, et al., 2012). The data of this work indicates an increase in di-acylated lipoproteins in low pH as well as high salt concentrations. Technical differences might account for differences in results. Future work will show whether this is the case.

A weakness of this work is the unknown absolute gene and protein expression. Since only the relative gene expression was measured, a strong decrease can still mean a relatively high expression. In that case, *lnsA* and *lnsB* could have decreased significantly, but the amount of functioning protein on acylating lipoproteins might still have been enough to not cause a change in lipoprotein lipidation. Furthermore, LnsA and LnsB might not be the only factors involved in tri-acylating lipoproteins and other factors might play a role under some conditions.

Antibiotics affect TLR2-dependent immune recognition of *S. aureus* in different ways (Wolf et al., 2017). On the one hand, cell wall active antibiotics disrupt cell wall integrity, which facilitates intra- and extracellular recognition of PAMPs that become better accessible in the cell and are released into the extracellular space. Penicillin, amongst others, increased TLR2-mediated cytokine release by liberating immunostimulatory lipoproteins (Hilmi et al., 2014). On the other hand, antibiotics at subinhibitory concentrations represent a stress signal and thus affect bacterial gene regulation causing an altered TLR2 response. As reported earlier, β-lactam-antibiotics at subinhibitory concentrations modulated gene expression by upregulating the virulence regulator SarA, leading to an increased transcription of lipoprotein-like genes as part of the stress response and finally a stronger TLR2-dependent immune recognition (Shang et al., 2019). However, in this work, bacterial growth in the presence of subinhibitory ampicillin did not significantly affect the expression of *lnsA* or *lnsB* (Figure 3.8), nor did it change recognition by TLRs (Figure 3.15, A3). The reason for this discrepancy might be related to differences in the experimental setup and kinetics as well as the selected strains and their susceptibility to the antibiotics tested.

Despite the unresolved causality of the changes in favored TLR engagement in different conditions, the presented *in vitro* data clearly showed changes in the affinity to TLR2 and its heterodimerization receptors as a consequence of exposure of staphylococci to different environmental conditions. This reflects a change in innate immune recognition of the same pathogen. In this study, the internalized, in Europe widely distributed, version of TLR1 (TLR1 602S) was used mainly for control purposes. However, observing an attenuated TLR1 signal, with the knowledge of most Europeans not carrying TLR1 on their immune cells, raises questions concerning evolutionary advantages and direct consequences for colonization and infection. TLR1 has been postulated to be involved in tolerance and immunosuppression because TLR1 ligand Pam_3CSK_4 has been shown to initiate the differentiation of monocytic myeloid-derived suppressor cells into immunosuppressive M2-like macrophages creating an immunosuppressive environment (Wang et al., 2015). Also, TLR1 activation in the gut has been shown to attenuate immune activation and chronic inflammation (Kamdar et al., 2018).

Future *in vivo* experiments are needed to understand the consequences of the observed switches between TLR2/1 and TLR2/6 signal in colonization and infection.

5 Summary

The analysis of 30 clinical *S. aureus* isolates showed a great diversity concerning their genetic origins, disease manifestation and virulence factor expression. While the *lnsA* locus appeared highly conserved, the *lnsB* locus showed greater diversity leading to several non-conserved amino acid substitutions. However, this diversity was not associated with variation in the expression of the genes under stress-inducing conditions low pH and high salt concentrations. Both genes were strongly downregulated in these conditions. Not much is known about the regulation of *lnsA* and *lnsB*. A clear correlation could be observed between *lnsA* and *lnsB* expression, despite the different genomic loci of both genes. Notably, the extent of stress-induced decrease in *lnsA* and *lnsB* expression observed at the level of an isolate was not equivalent in the high salt and low pH conditions, suggesting that expression of these genes in low pH and high salt concentrations might be regulated by distinct factors. Since *lnsA* and *lnsB* are responsible for the tri-acylation of *S. aureus* lipoproteins, a decreased expression was expected to cause a stronger TLR2/6 signal indicating di-acylated lipoproteins in line with an impaired TLR2/1 signal indicating tri-acylated lipoproteins. TLR2 heterodimer binding was altered resulting in stronger TLR2/6 signal and an attenuated TLR2/1 signal under cellular stress. Although the observed changes in TLR specificity were not as clear as previously described with *lnsA* and *lnsB* double knockouts, the data support the altered TLR2 response. Furthermore, the expression of *lnsA* and *lnsB* as well as the specificity of *S. aureus* lipoproteins as TLR1/2/6 ligands appears highly conserved. Despite their genetic diversity, no sub-populations of isolates behaving differently could be observed. Thus, strain origin and acquired virulence factors do not affect lipoprotein modification and recognition by human TLR1/2/6. Since this work was done using a representative collection of isolates, the drawing conclusion seems transferable to other *S. aureus* isolates but *in vivo* experiments are warranted to explore the significance of these *in vitro* findings in colonization and infection.

6 Annex

Table 6.1: Antibiotic susceptibility testing of *S. aureus* isolates 1-14 determined by minimal inhibitory concentration testing. R = resistant; I = intermediate; S = susceptible.

	CF014	CF018	CF031	CF173	FB002	FB004	INV001	INV005	INV058	INV075	INV078	INV091	INV099	INV100
Clindamycin	S	S	R	R	S	S	R	R	S	R	R	S	R	S
Daptomycin	S	S	S	S	S	S	S	S	S	S	R	S	S	S
Erythromycin	R	S	R	R	S	S	R	R	S	R	R	S	R	I
Erythromycin/Clindamycin	R	S	R	R	S	S	R	R	S	R	R	S	R	S
Fosfomycin	S	S	R	R	S	S	S	S	S	S	S	S	S	S
Fusidic acid	S	R	S	S	S	S	S	S	S	S	S	S	S	S
Gentamicin	S	R	S	S	S	S	S	S	S	S	S	S	S	S
Gentamicin high level	S	S	S	S	S	S	S	S	S	S	S	S	S	S
Linezolid	S	S	S	S	S	S	S	S	S	S	S	S	S	S
Moxifloxacin	S	S	R	R	S	S	R	R	S	R	R	S	S	S
Mupirocin	S	S	S	S	S	S	S	S	I	S	S	S	S	S
Rifampicin	S	S	S	S	S	S	S	S	S	S	S	S	S	S
Synercid	S	S	S	S	S	S	S	S	S	S	S	S	S	S
Teicoplanin	S	S	S	S	S	S	S	S	S	S	S	S	S	S
Tigecycline	S	S	S	S	S	S	S	S	S	S	S	S	S	S
Trimethoprim/Sulfmethoxazole	S	S	S	S	S	S	S	S	S	S	S	S	S	S
Vancomycin	S	S	S	S	S	S	S	S	S	S	S	S	S	S

Table 6.2: Antibiotic susceptibility testing of *S. aureus* isolates 15-28 determined by minimal inhibitory concentration testing. R = resistant; I = intermediate; S = susceptible.

	INV101	INV108	INV109	INV117	INV120	INV130	INV144	INV148	INV162	INV172	INV179	INV195	INV198	INV202
Clindamycin	S	S	S	S	S	R	S	S	S	S	S	R	S	S
Daptomycin	S	S	S	S	S	S	S	S	S	S	S	S	S	S
Erythromycin	S	S	S	S	R	R	R	S	I	R	S	R	S	S
Erythromycin/Clindamycin	S	S	S	S	R	R	R	S	S	R	S	R	S	S
Fosfomycin	S	S	S	S	S	S	S	S	S	S	S	R	S	S
Fusidic acid	S	S	S	S	S	S	S	S	S	S	R	S	S	S
Gentamicin	S	S	S	S	S	S	S	S	S	S	S	R	S	S
Gentamicin high level	S	S	S	S	S	S	S	S	S	S	S	S	S	S
Linezolid	S	S	S	S	S	S	S	S	S	S	S	S	S	S
Moxifloxacin	R	S	S	S	S	R	S	S	S	S	S	R	S	S
Mupirocin	S	S	S	S	S	S	I	S	S	S	S	S	S	S
Rifampicin	S	S	S	S	S	S	S	S	S	S	S	R	S	S
Synercid	S	S	S	S	S	S	S	S	S	S	S	S	S	S
Teicoplanin	S	S	S	S	S	S	S	S	S	S	S	S	S	S
Tigecycline	S	S	S	S	S	S	S	S	S	S	S	S	S	S
Trimethoprim/Sulfmethoxazole	S	S	S	S	S	S	S	S	S	S	S	S	S	S
Vancomycin	S	S	S	S	S	S	S	S	S	S	S	S	S	S

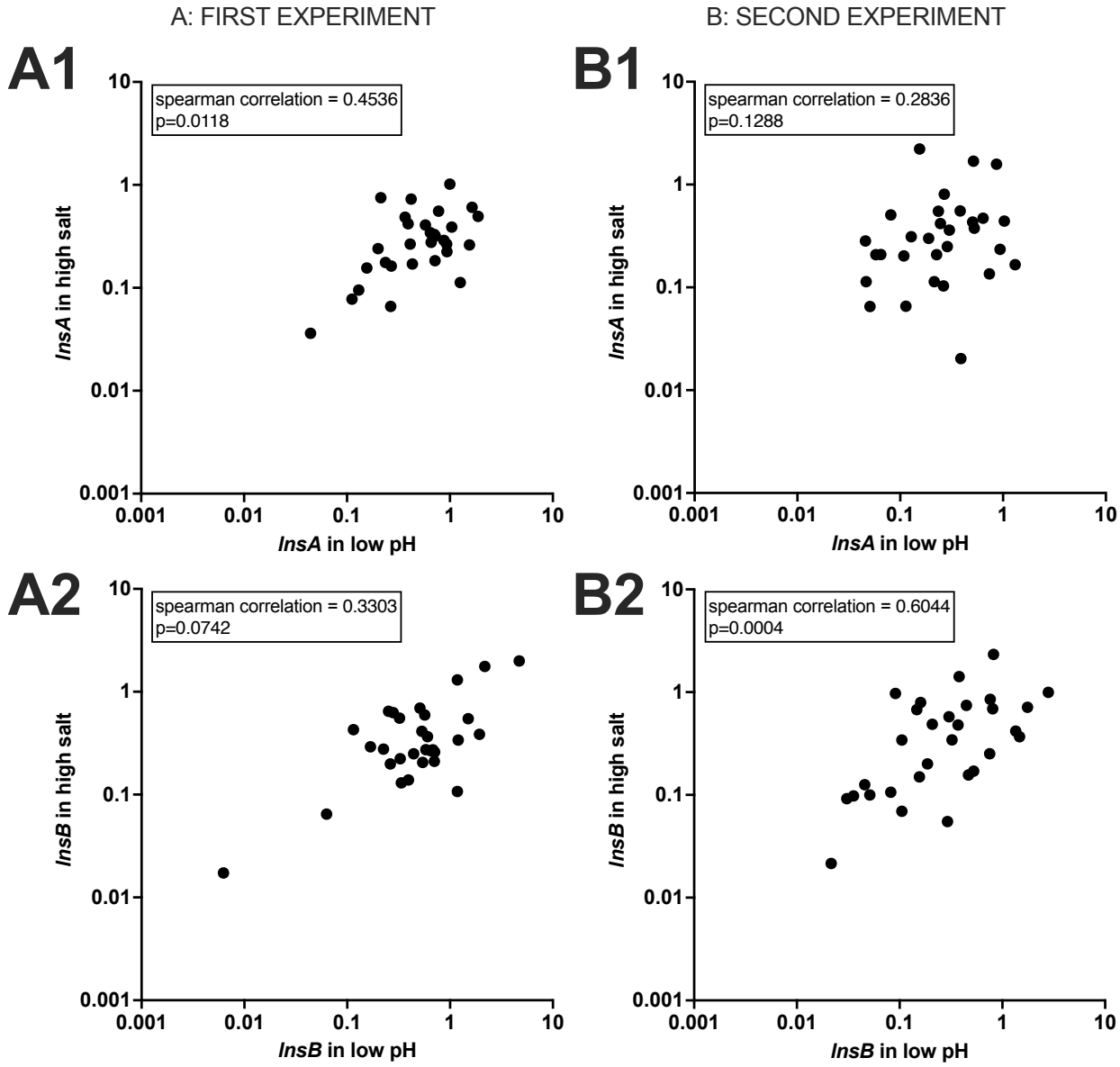

Figure 6.1: Correlation graphs of *InsA* and *InsB* under different conditions. A1 and B1 show the expression of *InsA* in *S. aureus* isolates grown in low pH (pH 5.5) as relative expression to the expression in isolates grown in neutral pH (pH 7.3) on the x-axis compared to the expression of *InsA* in *S. aureus* isolates grown in high salt concentrations (1 M NaCl) as relative expression to the expression in bacteria grown in low salt concentrations (0.086 M NaCl) on the y-axis. A2 and B2 show the expression for *InsB*. Graphs A and B derive from independent experiments.

7 List of figures

8 List of tables

9 References

An Diep, B., Gill, S. R., Chang, R. F., HaiVan Phan, T., Chen, J. H., Davidson, M. G., Lin, F., Lin, J., Carleton, H. A., Mongodin, E. F., Sensabaugh, G. F., & Perdreau-Remington, F. (2006). Complete genome sequence of USA300 an epidemic clone of. *Lancet*.

Asanuma, M., Kurokawa, K., Ichikawa, R., Ryu, K. H., Chae, J. H., Dohmae, N., Lee, B. L., & Nakayama, H. (2011). Structural evidence of α-aminoacylated lipoproteins of Staphylococcus aureus. *FEBS Journal*, *278*(5), 716–728. https://doi.org/10.1111/j.1742-4658.2010.07990.x

Bush, K., & Bradford, P. A. (2016). β-lactams and β-lactamase inhibitors: An overview. *Cold Spring Harbor Perspectives in Medicine*, *6*(8). https://doi.org/10.1101/cshperspect.a025247

Chambers, H. F., & DeLeo, F. R. (2009). Waves of resistance: Staphylococcus aureus in the antibiotic era. In *Nature Reviews Microbiology* (Vol. 7, Issue 9, pp. 629–641). https://doi.org/10.1038/nrmicro2200

Chen, X., & Alonzo, F. (2019). Bacterial lipolysis of immune-activating ligands promotes evasion of innate defenses. *Proceedings of the National Academy of Sciences of the United States of America*, *116*(9), 3764–3773. https://doi.org/10.1073/pnas.1817248116

Crossley, B. M., Bai, J., Glaser, A., Maes, R., Porter, E., Killian, M. L., Clement, T., & Toohey-Kurth, K. (2020). Guidelines for Sanger sequencing and molecular assay monitoring. *Journal of Veterinary Diagnostic Investigation*, *32*(6), 767–775. https://doi.org/10.1177/1040638720905833

Enright, M. C., Day, N. P. J., Davies, C. E., Peacock, S. J., & Spratt, B. G. (2000). Multilocus Sequence Typing for Characterization of Methicillin-Resistant and Methicillin-Susceptible Clones of Staphylococcus aureus. In *JOURNAL OF CLINICAL MICROBIOLOGY* (Vol. 38, Issue 3). http://mlst.zoo.ox.ac.uk

Feng, Y., Ming, T., Zhou, J., Lu, C., Wang, R., & Su, X. (2022). The Response and Survival Mechanisms of Staphylococcus aureus under High Salinity Stress in Salted Foods. *Foods*, *11*(10). https://doi.org/10.3390/foods11101503

Gardiner, J. H., Komazin, G., Matsuo, M., Cole, K., Götz, F., & Meredith, T. C. (2020). *Lipoprotein N-Acylation in Staphylococcus aureus Is Catalyzed by a Two-Component Acyl Transferase System*. http://mbio.asm.org/

Goss, C. H., & Muhlebach, M. S. (2011). Review: Staphylococcus aureus and MRSA in cystic fibrosis. In *Journal of Cystic Fibrosis* (Vol. 10, Issue 5, pp. 298–306). https://doi.org/10.1016/j.jcf.2011.06.002

Grayczyk, J. P., Harvey, C. J., Laczkovich, I., & Alonzo, F. (2017). A Lipoylated Metabolic Protein Released by Staphylococcus aureus Suppresses Macrophage Activation. *Cell Host and Microbe*, *22*(5), 678-687.e9. https://doi.org/10.1016/j.chom.2017.09.004

Hilmi, D., Doctoral thesis: The impact of *S. aureus* intra-strain and intra-species variability on immune recognition and functional properties, Heidelberg University, 2013

Hilmi, D., Master thesis: The impact of *S. aureus* virulence factors on immune recognition, Heidelberg University, 2010

Hilmi, D., Parcina, M., Stollewerk, D., Ostrop, J., Josten, M., Meilaender, A., Zaehringer, U., Wichelhaus, T. A., Bierbaum, G., Heeg, K., Wolz, C., & Bekeredjian-Ding, I. (2014). Heterogeneity of host TLR2 stimulation by Staphylocoocus aureus isolates. *PLoS ONE*, *9*(5). https://doi.org/10.1371/journal.pone.0096416

Hornbeck, P. V. (2015). Enzyme-linked immunosorbent assays. *Current Protocols in Immunology*, *2015*, 2.1.1-2.1.23. https://doi.org/10.1002/0471142735.im0201s110

Hu, J., Han, J., Li, H., Zhang, X., Liu, L. L., Chen, F., & Zeng, B. (2018). Human Embryonic Kidney 293 Cells: A Vehicle for Biopharmaceutical Manufacturing, Structural Biology, and Electrophysiology. In *Cells Tissues Organs* (Vol. 205, Issue 1, pp. 1–8). S. Karger AG. https://doi.org/10.1159/000485501

Jin, M. S., Kim, S. E., Heo, J. Y., Lee, M. E., Kim, H. M., Paik, S. G., Lee, H., & Lee, J. O. (2007). Crystal Structure of the TLR1-TLR2 Heterodimer Induced by Binding of a Tri-Acylated Lipopeptide. *Cell*, *130*(6), 1071–1082. https://doi.org/10.1016/j.cell.2007.09.008

Johnson, C. M., Lyle, E. A., Omueti, K. O., Stepensky, V. A., Yegin, O., Alpsoy, E., Hamann, L., Schumann, R. R., & Tapping, R. I. (2007). Cutting Edge: A Common Polymorphism Impairs Cell Surface Trafficking and Functional Responses of TLR1 but Protects against Leprosy. *The Journal of Immunology*, *178*(12), 7520–7524. https://doi.org/10.4049/jimmunol.178.12.7520

Kamdar, K., Johnson, A. M. F., Chac, D., Myers, K., Kulur, V., Truevillian, K., & DePaolo, R. W. (2018). Innate Recognition of the Microbiota by TLR1 Promotes Epithelial Homeostasis and Prevents Chronic Inflammation. *The Journal of Immunology*, *201*(1), 230–242. https://doi.org/10.4049/jimmunol.1701216

Kang, J. Y., Nan, X., Jin, M. S., Youn, S. J., Ryu, Y. H., Mah, S., Han, S. H., Lee, H., Paik, S. G., & Lee, J. O. (2009). Recognition of Lipopeptide Patterns by Toll-like Receptor 2-Toll-like Receptor 6 Heterodimer. *Immunity*, *31*(6), 873–884. https://doi.org/10.1016/j.immuni.2009.09.018

Köck, R., Mellmann, A., Schaumburg, F., Friedrich, A. W., Kipp, F., & Becker, K. (2011). The Epidemiology of Methicillin-Resistant Staphylococcus aureus (MRSA) in Germany. *Deutsches Ärzteblatt International*. https://doi.org/10.3238/arztebl.2011.0761

Kurokawa, K., Kim, M. S., Ichikawa, R., Ryu, K. H., Dohmae, N., Nakayama, H., & Lee, B. L. (2012). Environment-mediated accumulation of diacyl lipoproteins over their

triacyl counterparts in Staphylococcus aureus. *Journal of Bacteriology*, *194*(13), 3299–3306. https://doi.org/10.1128/JB.00314-12

Kurokawa, K., Lee, H., Roh, K. B., Asanuma, M., Kim, Y. S., Nakayama, H., Shiratsuchi, A., Choi, Y., Takeuchi, O., Kang, H. J., Dohmae, N., Nakanishi, Y., Akira, S., Sekimizu, K., & Lee, B. L. (2009). The triacylated ATP binding cluster transporter substrate-binding lipoprotein of Staphylococcus aureus functions as a native ligand for toll-like receptor 2. *Journal of Biological Chemistry*, *284*(13), 8406–8411. https://doi.org/10.1074/jbc.M809618200

Kurokawa, K., Ryu, K. H., Ichikawa, R., Masuda, A., Kim, M. S., Lee, H., Chae, J. H., Shimizu, T., Saitoh, T., Kuwano, K., Akira, S., Dohmae, N., Nakayama, H., & Lee, B. L. (2012). Novel bacterial lipoprotein structures conserved in low-GC content gram-positive bacteria are recognized by toll-like receptor 2. *Journal of Biological Chemistry*, *287*(16), 13170–13181. https://doi.org/10.1074/jbc.M111.292235

Lowy, F. D. (1998). Staphylococccus aureus infections. *The New England Journal of Medicine*.

Nakayama, H., Kurokawa, K., & Lee, B. L. (2012). Lipoproteins in bacteria: Structures and biosynthetic pathways. In *FEBS Journal* (Vol. 279, Issue 23, pp. 4247–4268). https://doi.org/10.1111/febs.12041

National Center for Biotechnology Information, 2022: Reference SNP (rs) Report rs5743618. https://www.ncbi.nlm.nih.gov/snp/rs5743618 (access date: 19.11.2023)

Paterson, G. K., Larsen, A. R., Robb, A., Edwards, G. E., Pennycott, T. W., Foster, G., Mot, D., Hermans, K., Baert, K., Peacock, S. J., Parkhill, J., Zadoks, R. N., & Holmes, M. A. (2012). The newly described mecA homologue, mecALGA251, is present in methicillin-resistant Staphylococcus aureus isolates from a diverse range of host species. *Journal of Antimicrobial Chemotherapy*, *67*(12), 2809–2813. https://doi.org/10.1093/jac/dks329

Pichon, B., Hill, R., Laurent, F., Larsen, A. R., Skov, R. L., Holmes, M., Edwards, G. F., Teale, C., & Kearns, A. M. (2012). Development of a real-time quadruplex PCR assay for simultaneous detection of nuc, panton-valentine leucocidin (PVL), mecA and homologue mecALGA251. *Journal of Antimicrobial Chemotherapy*, *67*(10), 2338–2341. https://doi.org/10.1093/jac/dks221

Schmaler, M., Jann, N. J., Götz, F., & Landmann, R. (2010). Staphylococcal lipoproteins and their role in bacterial survival in mice. In *International Journal of Medical Microbiology* (Vol. 300, Issues 2–3, pp. 155–160). https://doi.org/10.1016/j.ijmm.2009.08.018

Shang, W., Rao, Y., Zheng, Y., Yang, Y., Hu, Q., Hu, Z., Yuan, J., Peng, H., Xiong, K., Tan, L., Li, S., Zhu, J., Li, M., Hu, X., Mao, X., & Rao, X. (2019). β-Lactam antibiotics enhance the pathogenicity of methicillin-resistant Staphylococcus aureus via SarA-controlled lipoprotein-like cluster expression. *MBio*, *10*(3). https://doi.org/10.1128/mBio.00880-19

Skevaki, C., Pararas, M., Kostelidou, K., Tsakris, A., & Routsias, J. G. (2015). Single nucleotide polymorphisms of Toll-like receptors and susceptibility to infectious diseases. *Clinical and Experimental Immunology*, *180*(2), 165–177. https://doi.org/10.1111/cei.12578

Smithers, L., Olatunji, S., & Caffrey, M. (2021). Bacterial Lipoprotein Posttranslational Modifications. New Insights and Opportunities for Antibiotic and Vaccine Development. In *Frontiers in Microbiology* (Vol. 12). Frontiers Media S.A. https://doi.org/10.3389/fmicb.2021.788445

Takeuchi, O., Hoshino, K., & Akira, S. (2000). Cutting Edge: TLR2-Deficient and MyD88-Deficient Mice Are Highly Susceptible to Staphylococcus aureus Infection . *The Journal of Immunology*, *165*(10), 5392–5396. https://doi.org/10.4049/jimmunol.165.10.5392

Takeuchi, O., Hoshino, K., Kawai, T., Sanjo, H., Takada, H., Ogawa, T., Takeda, K., & Akira, S. (1999). Differential Roles of TLR2 and TLR4 in Recognition of Gram-Negative and Gram-Positive Bacterial Cell Wall Components to participate in the antibacterial host defense but not in the antifungal response, indicating that particular pathogens induce specific antimicrobial responses in Drosophila through the selective activation of the Toll pathways (Lemaitre et al. In *Technology of Japan Science* (Vol. 11).

Tawaratsumida, K., Furuyashiki, M., Katsumoto, M., Fujimoto, Y., Fukase, K., Suda, Y., & Hashimoto, M. (2009). Characterization of N-terminal structure of TLR2-activating lipoprotein in Staphylococcus aureus. *Journal of Biological Chemistry*, *284*(14), 9147–9152. https://doi.org/10.1074/jbc.M900429200

Tenover, F. C., McDougal, L. K., Goering, R. V., Killgore, G., Projan, S. J., Patel, J. B., & Dunman, P. M. (2006). Characterization of a strain of community-associated methicillin-resistant Staphylococcus aureus widely disseminated in the United States. *Journal of Clinical Microbiology*, *44*(1), 108–118. https://doi.org/10.1128/JCM.44.1.108-118.2006

van Hal, S. J., Jensen, S. O., Vaska, V. L., Espedido, B. A., Paterson, D. L., & Gosbell, I. B. (2012). Predictors of mortality in staphylococcus aureus bacteremia. In *Clinical Microbiology Reviews* (Vol. 25, Issue 2, pp. 362–386). https://doi.org/10.1128/CMR.05022-11

VanGuilder, H. D., Vrana, K. E., & Freeman, W. M. (2008). Twenty-five years of quantitative PCR for gene expression analysis. In *BioTechniques* (Vol. 44, Issue 5, pp. 619–626). https://doi.org/10.2144/000112776

Wang, J., Shirota, Y., Bayik, D., Shirota, H., Tross, D., Gulley, J. L., Wood, L. V., Berzofsky, J. A., & Klinman, D. M. (2015). Effect of TLR Agonists on the Differentiation and Function of Human Monocytic Myeloid-Derived Suppressor

Cells. *The Journal of Immunology*, *194*(9), 4215–4221. https://doi.org/10.4049/jimmunol.1402004

Wertheim, A. (2019). Regulation of Staphylococcus aureus Virulence. *Microbiology Spectrum*, *7*(2). https://doi.org/10.1128/microbiolspec.gpp3-0031-2018

Wertheim, H. F. L., Vos, M. C., Ott, A., Van Belkum, A., Voss, A., Kluytmans, J. A. J. W., Van Keulen, P. H. J., Vandenbroucke-Grauls, C. M. J. E., Meester, M. H. M., & Verbrugh, H. A. (2004). Risk and outcome of nosocomial Staphylococcus aureus bacteraemia in nasal carriers versus non-carriers. *Lancet*, *364*(9435), 703–705. https://doi.org/10.1016/S0140-6736(04)16897-9

Wertheim, H., Melles, D., Vos, M., van Leeuwen, W., van Belkum, A., Verbrugh HA, & Nouwen, J. (2005). The role of nasal carriage in Staphylococcus aureus infections. *Lancet Infect Dis*.

Wolf, A. J., Liu, G. Y., & Underhill, D. M. (2017). Inflammatory properties of antibiotic-treated bacteria. *Journal of Leukocyte Biology*, *101*(1), 127–134. https://doi.org/10.1189/jlb.4mr0316-153rr

10 Declaration of personal contribution

Prof. Dr. Isabelle Bekeredjian-Ding assigned the doctoral project, provided the topic, laboratory resources, infrastructure and funding. The lab work was supervised by Dr. Karen Huber (Paul-Ehrlich-Institute, Langen) and Priv.-Doz. Dr. Marijo Parcina (Institute for Medical Microbiology, Immunology and Parasitology, Bonn), respectively. I received technical assistance from Christoph Stein for several experiments that needed to be repeated after I had left the Paul-Ehrlich-Institute. MLST data was kindly povided by Dr. Karen Huber.

My independent contributions included designing and optimizing experiments, analyzing data and writing the dissertation. I also took initiative in developing methodological approaches and interpreting results, thus contributing substantially to the scientific outcomes of the project.

I declare, that I wrote this thesis myself. I did not make use of any sources or resources not mentioned within this thesis.

11 Acknowledgments

First, I thank Prof. Dr. med. Isabelle Bekeredjian-Ding for enabling this project, for giving me the chance to spend six months in Microbiology Division at Paul-Ehrlich-Institute and for the persistent support to date.

I thank Dr. Karen Huber for the dedicated supervision of this project, for supporting me on a daily basis and being reachable at any time.

I thank Christoph Stein for his committed support concerning technical questions and his help in the accomplishment of all experiments.

I thank the entire Microbiology Division at Paul-Ehrlich-Institute for the support.

I thank Priv.-Doz. Dr. Marijo Parcina for enabling experiments at the Institute for Medical Microbiology, Immunology and Parasitology in Bonn.

I thank my family for their support and understanding.

I thank the German Center for Infection Research for the financial support.